General Disclaimer

One or more of the Following Statements may affect this Document

- This document has been reproduced from the best copy furnished by the organizational source. It is being released in the interest of making available as much information as possible.

- This document may contain data, which exceeds the sheet parameters. It was furnished in this condition by the organizational source and is the best copy available.

- This document may contain tone-on-tone or color graphs, charts and/or pictures, which have been reproduced in black and white.

- This document is paginated as submitted by the original source.

- Portions of this document are not fully legible due to the historical nature of some of the material. However, it is the best reproduction available from the original submission.

NASA CR-141409

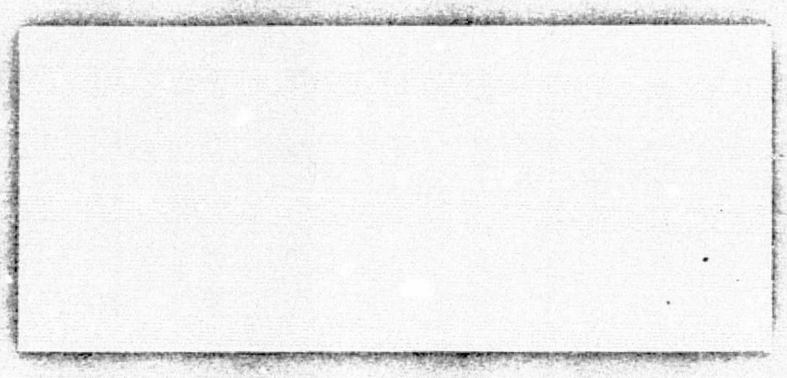

(NASA-CR-141409) MANSEE DATA ANALYSIS RESULTS (Wolf Research and Development Corp.) 89 p HC $5.00 CSCL 17G

N76-28213

Unclas
G3/04 47246

WOLF RESEARCH AND DEVELOPMENT CORPORATION

MANSEE
DATA ANALYSIS RESULTS

July 1975

Prepared For

NASA/Wallops
Wallops Flight Center
Wallops Island, Virginia 23337

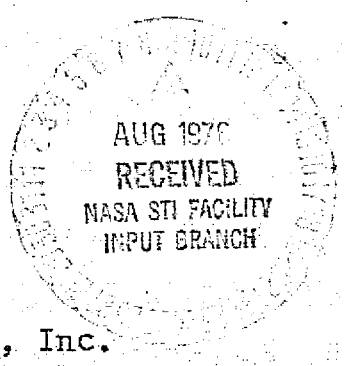

Prepared By

William Hatch
Bruce Gibbs

Wolf Research and Development Group
EG&G/Washington Analytical Services Center, Inc.
6801 Kenilworth Avenue
Riverdale, Maryland 20840

Planetary Sciences Department Report No. 006-75

TABLE OF CONTENTS

TABLE OF CONTENTS (Cont.)

LIST OF FIGURES

LIST OF TABLES

INTRODUCTION

Under Task II of contract NAS 6-2173 WOLF was responsible for assisting NASA/Wallops Flight Center in test planning, data reduction and analysis for the Marine Navigation Systems Evaluation Experiment (MANSEE). Under a previous contract, NAS 6-1942, WOLF developed the mathematical techniques to reduce and analyze the MANSEE data. See Appendix 1 for a mathematical description of this program. The results of this analysis are summarized in this report.

Section 1.0 describes the MANSEE test. Section 2.0 describes the navigation sensors which were exercised. Section 3.0 describes the ground truth instrumentation and the processing of ground truth data. Section 4.0 summarizes the residual statistics for individual navigation sensors. Here residuals were calculated by differencing the actual measurements with anticipated measurements computed from the ground truth trajectory. In most cases the ground truth trajectory was sufficiently accurate that these residuals could be attributed to navigation sensor measurement errors.

Section 5.0 presents some of the results obtained by using the SEAMAP program to filter data from the navigation sensors. The resultant filtered trajectories were differenced with the corresponding ground truth trajectories to obtain navigation position and velocity errors. Section 6.0 contains various conclusions and recommendations derived from the MANSEE effort.

Volume 2 contains the results from SINS data. This was made a separate volume because the results are classified.

SECTION 1.0
TEST DESCRIPTION AND CONDENSATION

The purpose of the MANSEE experiment was to exercise and evaluate representative navigation systems in current general usage by the maritime community. The test vehicle was the Apollo Range Ship USNS VANGUARD. Available navigation systems and navigation aid subsystems on-board the VANGUARD were supplemented with rented or borrowed navigation instrumentation so that representative systems from each genre were exercised. The test range was NASA's Wallops Flight Center, located at Wallops Island, Virginia, where precision tracking radars are available on the coast to provide the necessary "Ground Truth," or nominal trajectory of the ship (see Figure 1A).

The test was performed in three phases during June 1972. Phases one and three were instrument calibrations conducted at Port Canaveral, Florida, the home port of the VANGUARD. Phase two was the experiment operation, conducted on June 5, 6, and 7, 1972, in the immediate vicinity of Wallops Island, Virginia.

The design goal of the experiment procedure was to simultaneously exercise the various navigation systems on the ship through a series of varying trajectory geometrics and velocities. To maintain ground-truth control, the ship remained within line of sight of the land-based radars, a distance of 20-25 miles. To avoid shallow water, the ship remained 10-15 miles from shore. Thus, a sector of ocean approximately 15 miles by 25 miles was available for operations. The ship executed rectangular, crossing, and circular patterns at various velocities within the sector (see Figure 1B).

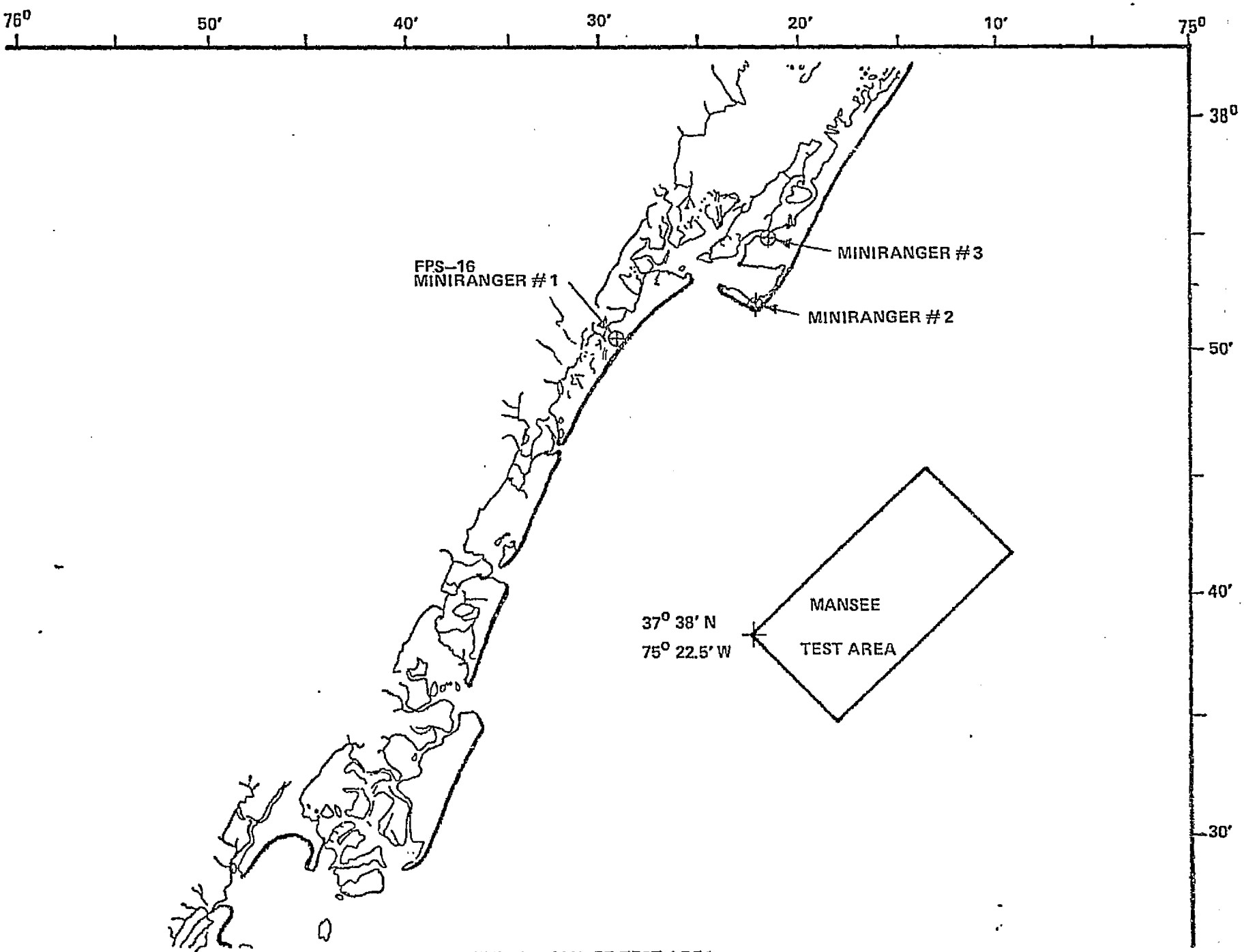

FIGURE 1A. MANSEE TEST AREA

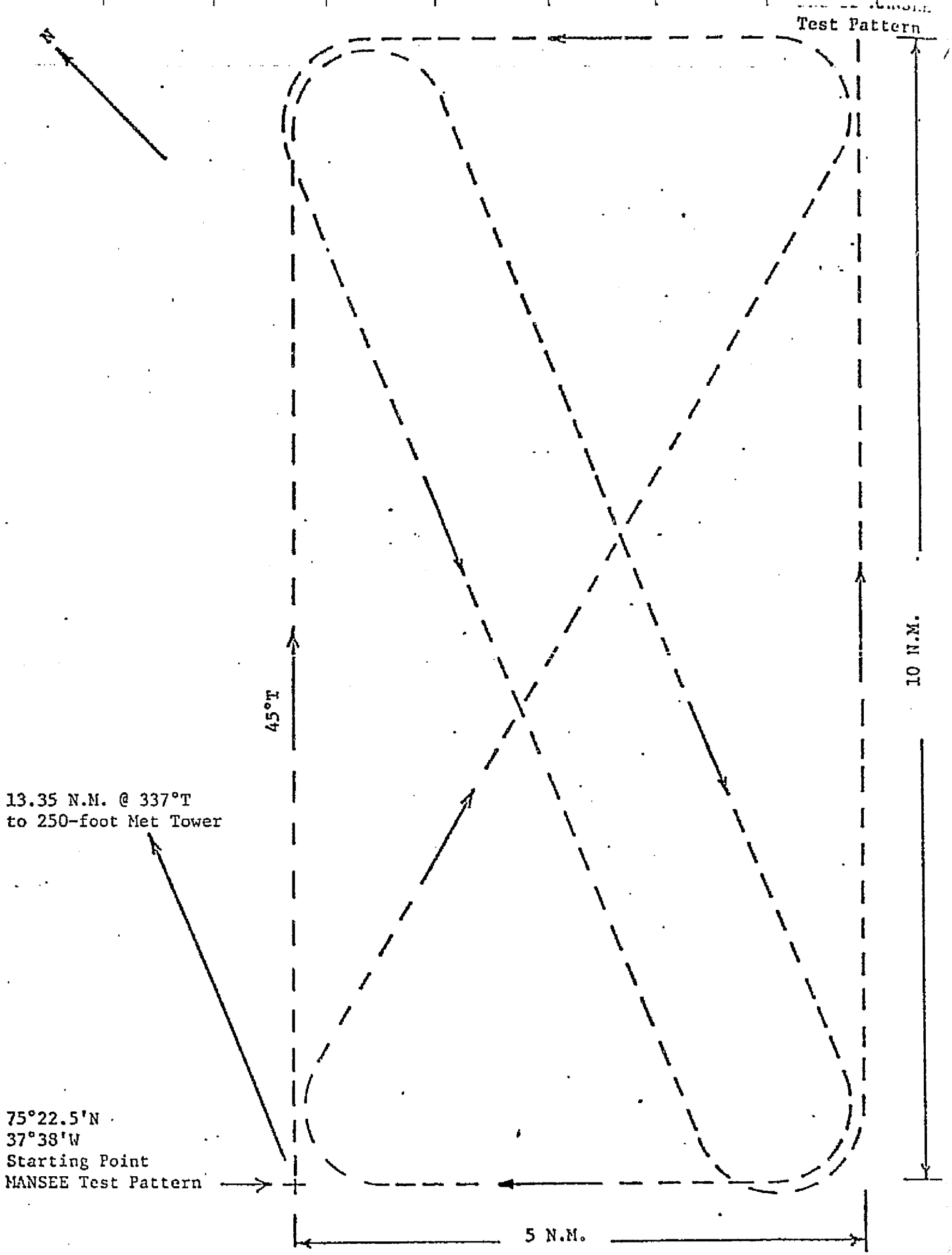
Test Pattern
N
45°T
10 N.M.
13.35 N.M. @ 337°T
to 250-foot Met Tower
75°22.5'N
37°38'W
Starting Point
MANSEE Test Pattern
5 N.M.

Figure 1B

The design goal of obtaining simultaneous data from all available sensors was met during several long periods of time during the test, with the exception of the relative velocity sensor. The EM Log was inoperable during the experiment. The available data set at the conclusion of the test contained in excess of one million independent position fixes for the three day operation - an amount more than adequate for sensor evaluation.

The performance of the navigation sensors was within or close to the nominal accuracy for all systems except Loran-C and the AN/SRN-9. Apparently the Z-channel of Loran-C locked up on the wrong cycle of the carrier producing a 2500 meter error. However, the Y-channel was accurate to within 24 meters (RSS). The usable data from the AN/SRN-9 consisted of only four points which is insufficient to state definite conclusions of its accuracy.

SECTION 2.0
INSTRUMENTATION

2.1 NAVIGATION SENSORS

The selection of the VANGUARD as a test vehicle was advantageous both from the standpoint of having a highly trained crew to operate the navigation systems, and having a complement of navigation sensors available, as the following list indicates:

1. LORAN-C Receiver
2. Inertial Navigation System (SINS)
3. Marine Star Tracker
4. Electro-Magnetic Velocity Log
5. Mark-19 Gyrocompass
6. SRN-9 Navy Navigation Satellite System Receiver

To this instrumentation set was added, through lease contracts or subcontracts, or loans from other government agencies, the following navigation sensors:

1. Raydist Navigator
2. Motorola Mini-Ranger
3. Omega Receiver

Detailed specifications on the above instrumentation are available from Wallops Station. A summary description of each system follows:

LORAN-C - The LORAN-C Receiver on the VANGUARD is a Collins SPN-38.

SINS - The inertial navigation system on the VANGUARD is a Sperry MK3 Mod 5. The system consists of four gyros and three accelerometers mounted on a stabilized platform, all of which are input to a MINDAC computer. The output from the MINDAC software consists of both gyro torqueing signals and the ship's position (latitude and longitude), velocities (north, east, vertical, and total horizontal) and heading.

MST - The Marine Star Tracker is a subsystem of the SINS. The instrument measures azimuth and elevation to stars for input to the MINDAC computer. The MINDAC software outputs ship's position (latitude and longitude) based on the star measurements.

EM LOG - This is a sensor on the VANGUARD for measuring ship's velocity relative to the surrounding water. The EM LOG was not operating during the MANSEE experiment.

MARK-19 GYROCOMPASS - The MARK-19 is a Sperry instrument. Measurements are ship's heading relative to the earth's spin-axis (true north), plus ship's roll and pitch angles relative to the local gravity vector.

SRN-9 RECEIVER - The AN/SRN-9 receiver on the VANGUARD was manufactured by ITT. The system receives and decodes transmissions from the Navy Navigation Satellite System. The measurements and satellite ephemeris are subsequently

processed (together with velocity and heading from the INS or the MK 19/EM LOG) in the UNIVAC 1230 computer on-board the ship. Output from the computer is a position fix (latitude and longitude) and standard deviation of the fix.

RAYDIST - The RAYDIST "T" navigator supplied by TELEDYNE HASTINGS - RAYDIST was used in the experiment. The navigator is a phase measuring receiver and was used in conjunction with the lower Chesapeake network of RAYDIST base stations. Measurements are transformed to latitude and longitude by determining the intersections of lines of position.

MINI-RANGER - The Motorola Mini-Ranger is a line-of-sight two-way range measuring system. The configuration used in this experiment had the range console, receiver/transmitter, and antenna on-board the VANGUARD, with three transponders mounted at surveyed locations on land.

OMEGA - The OMEGA receiver used in the experiment was a Dynel Electronics Model 200 loaned to NASA by the U.S. Navy.

2.2 "GROUND TRUTH" INSTRUMENTATION

"Ground Truth" instrumentation consisted of two AN/FPS-16 C-Band pulsed tracking radars, and two C-Band transponders. These radars, normally used to track rockets during launch and satellites in orbit, have been qualified

as geodetic instruments, with measurement accuracies of 2-3 meters in range and 15-30 arcseconds in angles. One radar is a permanent element of the VANGUARD's instrumentation complex, and a C-Band transponder was mounted on a tower on Wallops Island as a point source target for the radar to track. The other system is part of the Wallops Island radar complex, and a C-Band transponder was mounted on the VANGUARD's superstructure as a target for this radar. Detailed specifications on this instrumentation and its utilization are available from Wallops Flight Center.

SECTION 3.0
GROUND TRUTH DATA PROCESSING AND ANALYSIS

The data was subsampled by merging in time sequence alternate one hour segments of data on computer tapes. An analysis of all the ground truth data at a one per second rate on these tapes was conducted to validate the consistency of the ground truth measurements. The a priori error statistics (measurement noise and bias) for the radars from the pre-mission and post-mission calibrations were compared to the mission data.

The shipboard azimuth measurements contained a sinusoidal error having peak variations of 20 to 30 mils as compared to systematic errors of less than .1 mil for the land based radar. A probable explanation is that the ship's heading must be determined to a high degree of accuracy to process the measurement. Because of the wide discrepancies in data quality it was decided to use for ground truth data processing only shipboard range measurements and land based azimuth measurements. The error statistics used in all ground truth processing are as follows:

	Noise	Bias
RADAR RANGE (Ship)	$\pm$ 2 meters RMS	0 $\pm$ .5 meters
RADAR AZIMUTH (Land)	$\pm$ .2 mils RMS	0 $\pm$ .1 mils

The propagation of these errors along with possible survey uncertainties of $\pm$ 6 meters in latitude and longitude of the position of the land transponder yields a ground truth accuracy of the ship's trajectory of $\pm$ 5.2 meters (one sigma) relative to the position of the land radar. The ship's velocity is determined to $\pm$ .033 meters/second (one sigma) and the ship's heading to $\pm$ 1.0 degree (one sigma).

Figure 3.1 shows the ship trajectories with respect to the Wallops FPS-16 and Mini-Rangers. Figure 3.2 shows the RMS (predicted) position error vs. time for the 1422 data span when processing the radar data. The transponder location error one sigma contribution is 3.5 meters and the one sigma contribution due to measurement errors (noise and bias) is about 3.9 meters. Figure 3.3 shows the corresponding RMS velocity error vs. time.

Table 3.1 lists the radar residual statistics for all the data spans. Note that Wallops FPS-16 range (which was not weighted in the solution) agreed closely with the range measured by the Vangard FPS-16. The only exception was the 1612-1645 data span which had a mean range residual of 7.8 meters. It is not known why the bias was so large in this run since the bias was fairly constant throughout the run.

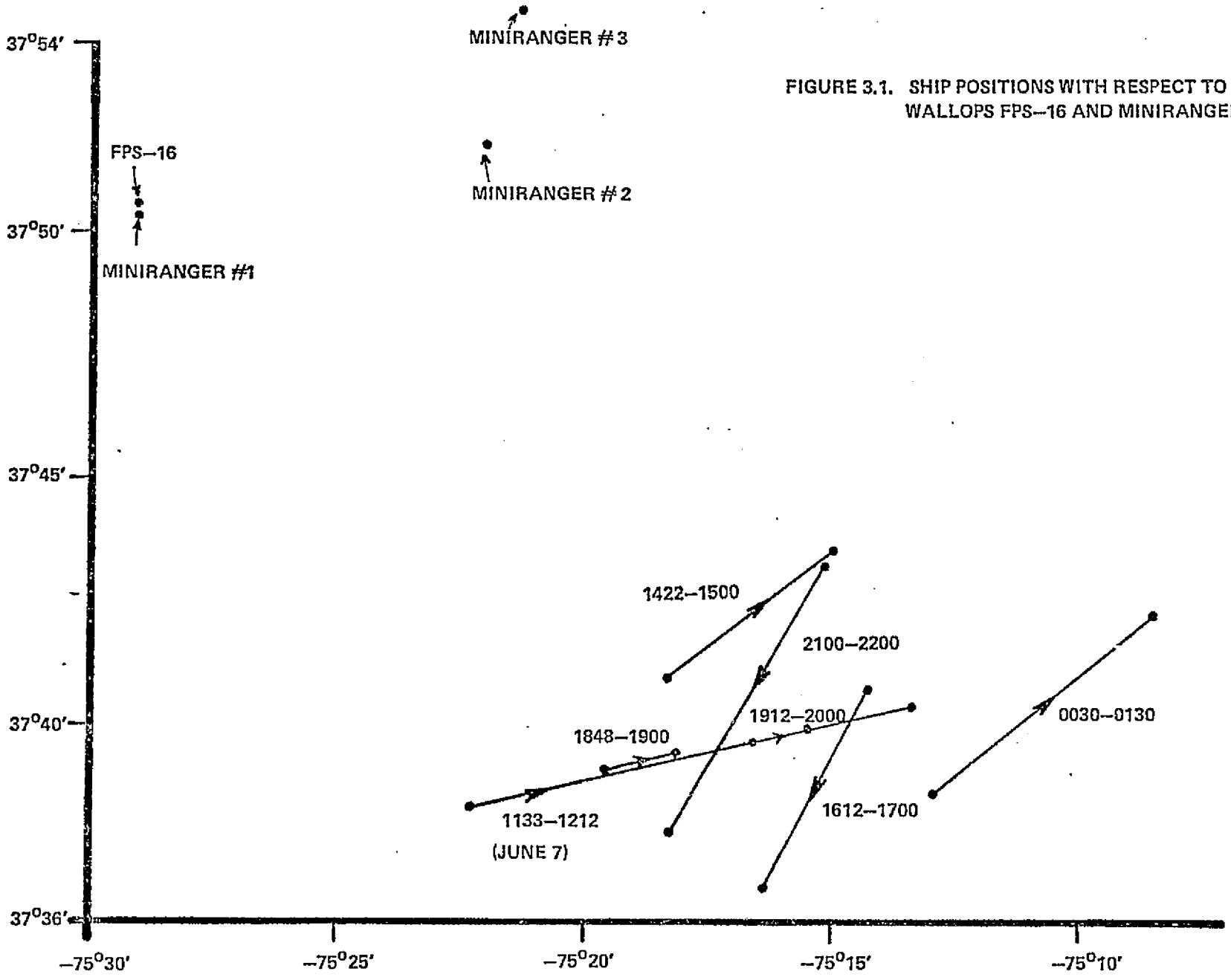

FIGURE 3.1. SHIP POSITIONS WITH RESPECT TO WALLOPS FPS–16 AND MINIRANGERS

Figure 3.2.

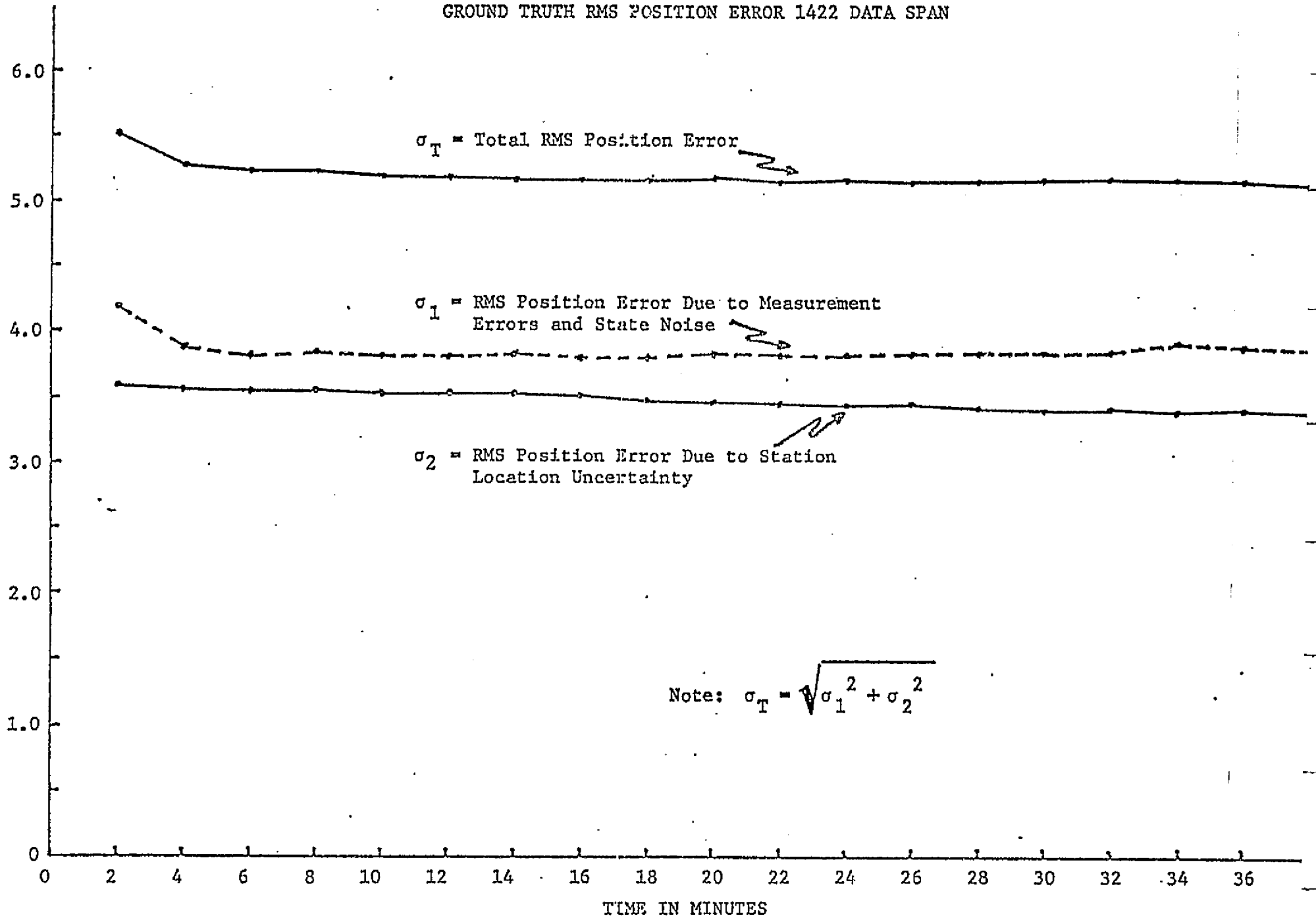
GROUND TRUTH RMS POSITION ERROR 1422 DATA SPAN
σ_T = Total RMS Position Error
σ_1 = RMS Position Error Due to Measurement Errors and State Noise
σ_2 = RMS Position Error Due to Station Location Uncertainty
Note: $\sigma_T = \sqrt{\sigma_1^2 + \sigma_2^2}$
RMS POSITION ERROR IN METERS
TIME IN MINUTES
0
1.0
2.0
3.0
4.0
5.0
6.0
0
2
4
6
8
10
12
14
16
18
20
22
24
26
28
30
32
34
36

Figure 3.3.

GROUND TRUTH RMS VELOCITY ERROR 1422 DATA SPAN

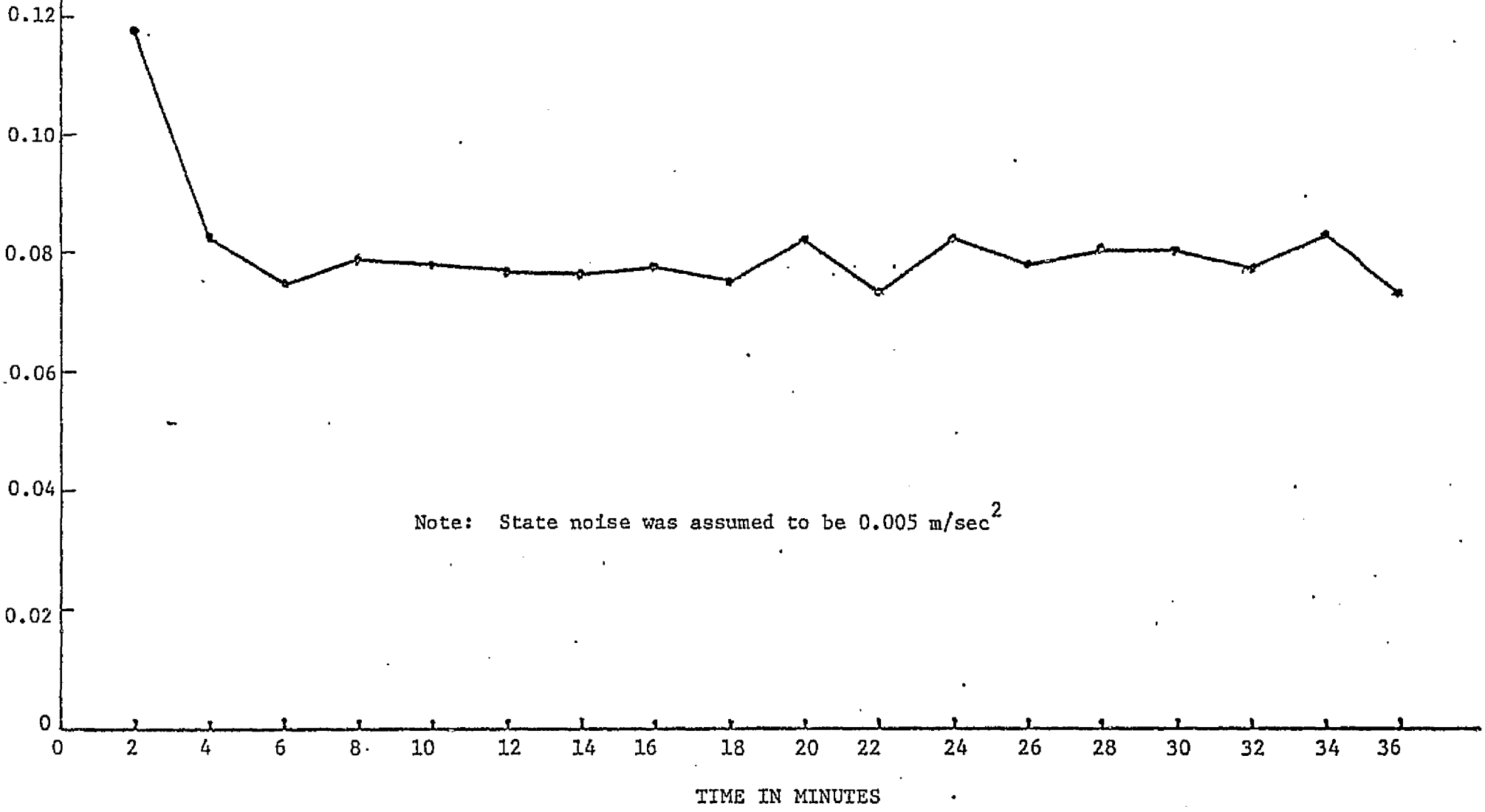

Note: State noise was assumed to be 0.005 m/sec^2

Table 3.1. Radar Residual Statistics For Individual Data Spans
(Meters and Mils)

Data Span	Wallops FPS-16					Vangard FPS-16				
	No. Data Points	Range Mean	Range Sigma	Azimuth Mean	Azimuth Sigma	No. Data Points	Range Mean	Range Sigma	Azimuth Mean	Azimuth Sigma
1422-1500Z	219	-0.1	2.0	-.01	0.25	211	0.0	1.9	1.93	12.74
1612-1645Z	152	7.8	3.0	0.00	0.45	145	0.09	2.0	22.03	24.30
1912-1940Z	150	0.4	1.8	-0.03	0.29	141	-0.1	1.9	-4.48	16.43
2100-2200Z	351	0.1	2.3	-0.01	0.57	351	0.0	1.9	-3.66	15.33
1133-1212Z (June 7)	225	3.4	4.1	-0.03	0.74	225	0.6	3.1	37.82	44.74
OVERALL	1097	1.8	2.8	-0.01	0.52	1073	0.1	2.2	9.50	25.35

SECTION 4.0
NAVIGATION SENSOR RESIDUALS

When processing multiple sensor data with the SEAMAP program, measurements from any sensor may be either used by the filter to improve the state estimate or processed in a residual analysis mode. For a ground truth run, data from both C-Band radars is used to update the state estimate while data from the navigation sensors is treated in the residual analysis mode.

A detailed residual analysis of the navigation sensors was performed for the following seven data spans:

June 6	0030Z - 0130Z
June 6	1422Z - 1500Z
June 6	1612Z - 1645Z
June 6	1846Z - 1900Z
June 6	1912Z - 2000Z
June 6	2100Z - 2200Z
June 7	1133Z - 1212Z

During these periods good quality ground truth data was available and most of the navigation sensors (except the EM Log) were operating.

While performing the data reduction, it was discovered that the location of the C-Band, radar transponder on board the ship was not input to the SEAMAP program. Since the transponder was 50.6 meters from the reference point of the ship, the computed ship position was in error by about 50 meters. Unfortunately, the data from the 0030-0130Z and 1846-1900Z spans were lost before the runs could be remade. The effect of this error on the results was computed (approximately) from the ship's heading, but results from these data spans are not listed here except for sensors which have errors much larger than 50 meters. The antenna locations of all other sensors were included in SEAMAP in all of the runs.

4.1 MEASUREMENT RESIDUAL MODEL

For each Navigation sensor, the measurement residual is computed as

$$\delta \underline{Y}_j = \underline{Y}_j - \hat{\underline{Y}}_j(\hat{\underline{X}}_j, \hat{\underline{s}}) \tag{4.1.1}$$

where:

$\underline{Y}_j$ = Actual measurement vector

$\hat{\underline{X}}_j$ = State vector estimated from C-Band radar data

$\hat{\underline{x}}$ = a priori values of sensor systematic error parameters.

If we express the measurement residual in terms of its component errors and neglect higher order terms:

$$\delta \underline{Y}_j = \underline{r}_j - A_j \delta \hat{\underline{s}} - M_j \delta \hat{\underline{X}}_j \tag{4.1.2}$$

where:

$\underline{r}_j$ = Random measurement error having zero mean and covariance matrix R_j

$\delta \hat{\underline{s}}$ = Error in a priori values of sensor systematic error parameters having zero mean and covariance matrix S

$\delta \hat{\underline{X}}_j$ = Error in state vector having zero mean and covariance matrix P_j

A_j = Partial derivatives of the measurement with respect to the systematic error parameters in $\underline{s}$

M_j = Partial derivatives of the measurement with respect to the adjusted parameters in $\underline{X}_j$.

When a sensor is treated in the residual analysis mode, these three error vectors are statistically independent.

In running SEAMAP, it is the usual practice to initiate residual analysis after the filter has converged and $\delta\hat{\underline{X}}_j$ is nearly constant.

For the residuals analyzed, A_j, M_j and $\delta\hat{\underline{X}}_j$ are nearly constant over a typical data span. In modeling the sensor errors, it is assumed that $\underline{s}$ is constant. Thus, each residual is hypothesized to be the sum of a random error plus two error terms that are constant over the data span. However, these constant terms may vary between data spans.

4.2 RESIDUAL STATISTICS

To determine the magnitude of the error terms, for each data span, the mean and standard deviation of each component of the residual vector were computed as

$$u_i = \frac{1}{n_i} \sum_{j=1}^{n_1} \delta y_{ij} \qquad (4.2.1)$$

$$\sigma_i = \sqrt{\frac{\sum_{j=1}^{n_i} (\delta y_{ij} - u_i)^2}{n_i - 1}}$$

where n_i is the number of residuals in the i^{th} data span ($i=1,2...7$) and δy_{ij} represents a component of the residual vector at time t_j during the i^{th} data span.

The overall mean and standard deviation for each residual component were computed as

$$u = \frac{1}{n} \sum_{i=1}^{7} n_i \, u_i \qquad (4.2.2)$$

$$\sigma = \sqrt{\frac{\sum_{i=1}^{7} (n_i - 1) \, \sigma_i^2 + \sum_{i=1}^{7} (u_i - u)^2}{n - 1}}$$

where:

$$n = \text{total number of data points} = \sum_{i=1}^{7} n_i \, .$$

Note that the overall standard deviation contains two components; one due to the scatter of residuals about the mean within the data span, and the second component due to the variability of the data span means about the overall mean. This second term is due to variations in the systematic residual components between data spans.

From equation 4.1.2 the covariance matrix associated with the mean residual vector for a given data span is given by

$$E(\underline{u}_i \underline{u}_i^T) = V_i = MPM^T + ASA^T + \frac{1}{n_i} R_i \qquad (4.2.3)$$

For the data spans analyzed, n_i was sufficiently large that the measurement noise contribution $\frac{1}{n_i} R_i$ could be neglected. The state error contribution MPM^T is analytically computed within SEAMAP. The presence of significant systematic measurement errors can be assessed by computing the ratio

$$g = \frac{u_i}{\sqrt{q_{n,n}}} \qquad (4.2.4)$$

where u_i is a residual mean and $q_{n,n}$ is the corresponding diagonal element of the matrix MPM^T.

For large n_i, if the mean measurement error is zero, the statistic "g" follows a normal distribution with mean zero and standard deviation one. Thus, if the magnitude of the residual mean is much larger than $\sqrt{q_{n,n}}$, we can say that the sensor bias is significantly different from zero and the value of u_i is the best available estimate of the corresponding element of $A\delta\underline{s}$. The standard deviation of this estimate is approximately $\sqrt{q_{nn}}$.

Under the assumptions that the error vectors $\delta \underline{X}_j$ and $\hat{\underline{s}}$ and the arrays A_j and M_j are nearly constant over a data span, the expected value of the residual standard deviation is the corresponding measurement noise standard deviation. These assumptions are clearly violated when the residual plots show significant trending or when the residual noise characteristics change during a data span.

Table 4.1 Navigation Sensors Overall Measurement Residual Statistics

Sensor	Measurement	Mean	Sigma	Sample Size
MINIRANGER 1	Range	-2.8 meters	3.6 meters	62
MINIRANGER 2	Range	-1.5 meters	4.4 meters	217
MINIRANGER 3	Range	-5.0 meters	5.3 meters	552
LORAN-C	Channel Y	-21 meters	12 meters	605
	Channel Z	-2581 meters	133 meters	956
MK-19 GYRO	Heading	3.3 degrees	2.3 degrees	1421
AN/SRN-9	Latitude	100 meters	551 meters	4
	Longitude	-170 meters	575 meters	4
OMEGA	Stations B-C	-1040 meters	611 meters	107
	Stations D-F	262 meters	589 meters	107
RAYDIST -T	Red Network	23.8 meters*	2.9 meters	1632
	Green Network	-11.1 meters*	3.5 meters	1631

*For Raydist, the mean residuals are primarily due to initialization error rather than system errors.

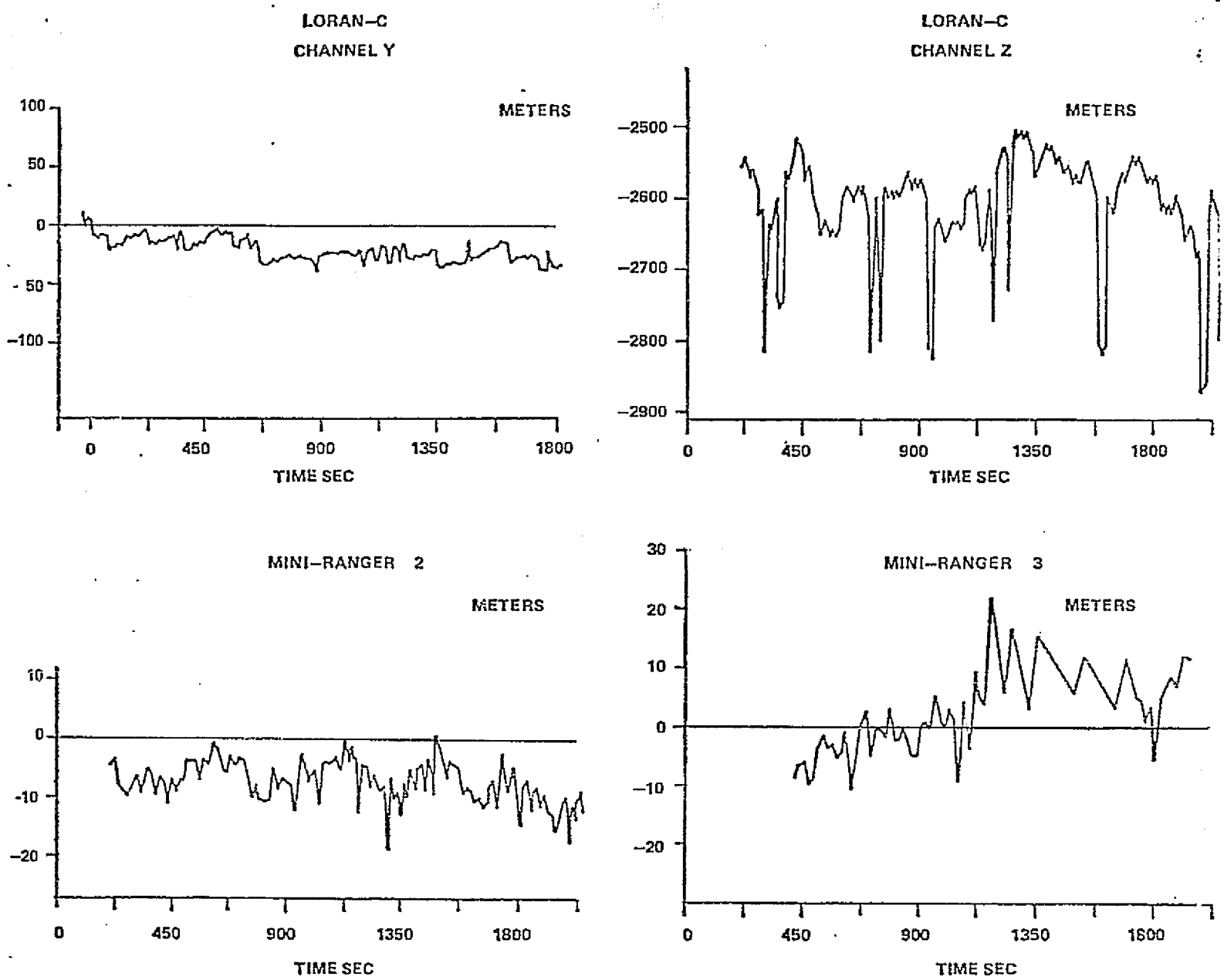

FIGURE 4.1. TYPICAL SEAMAP RESIDUAL PLOTS DAY 158 – 1422 DATA SPAN

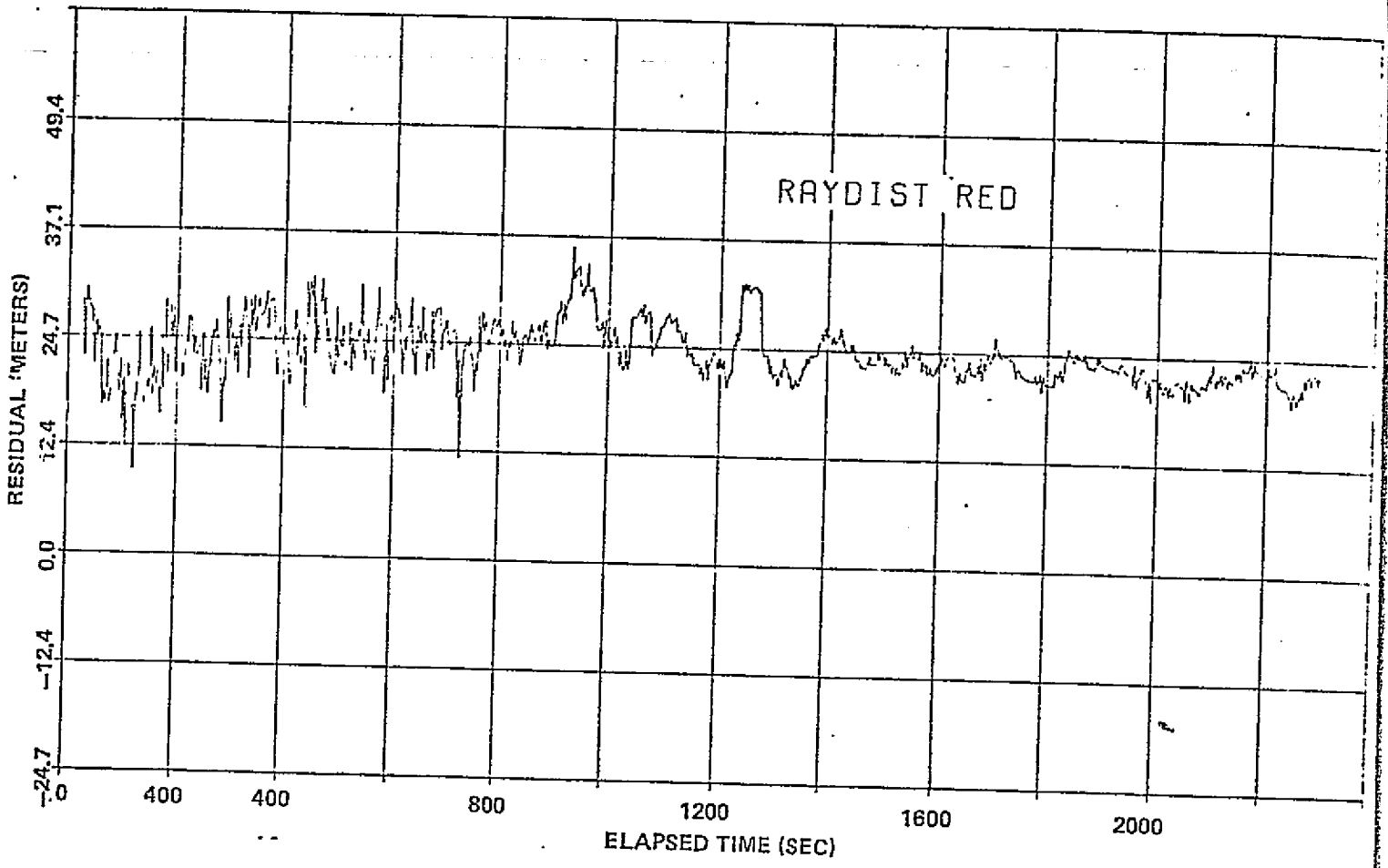

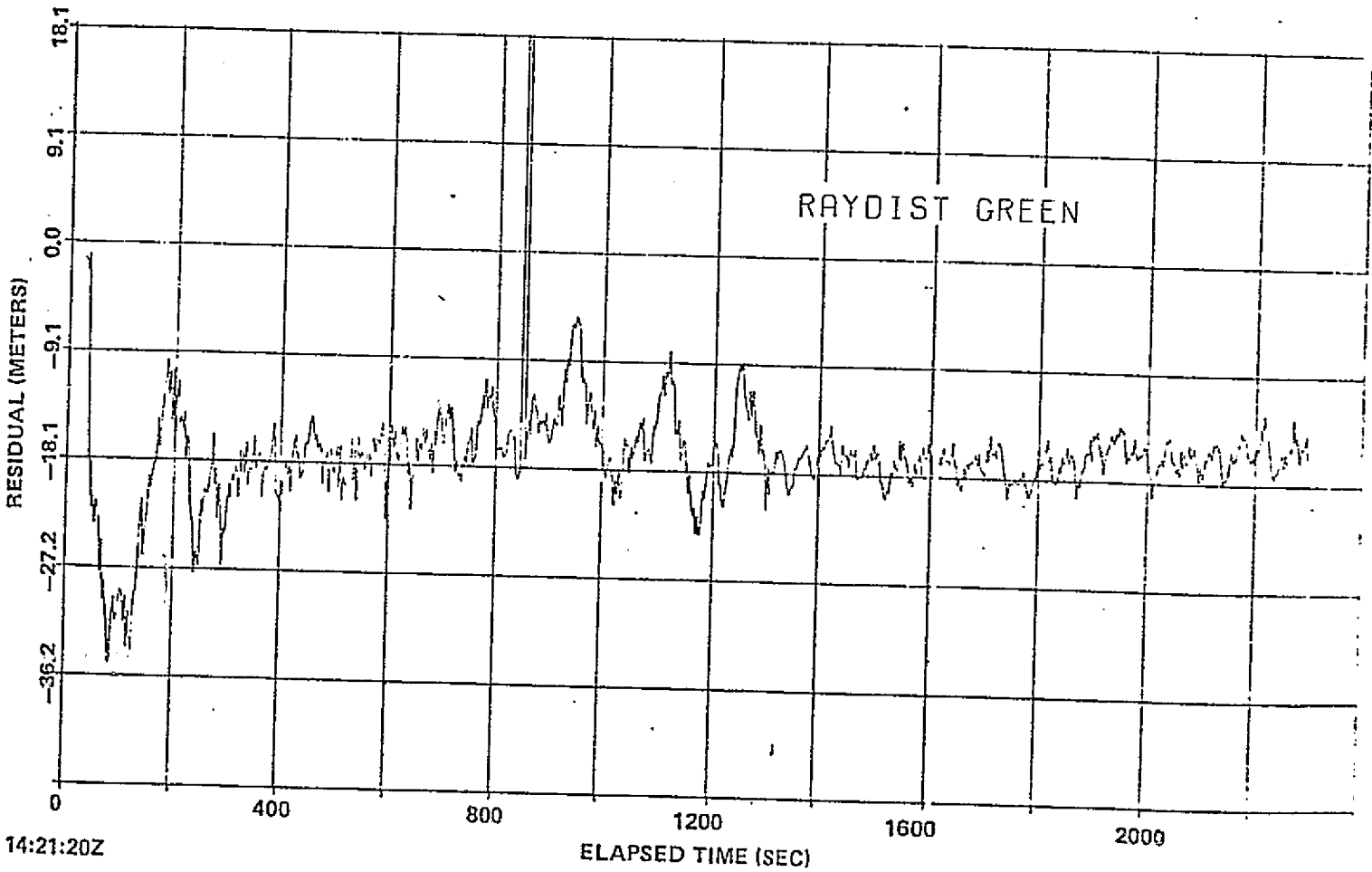

FIGURE 4.1. (Cont.) TYPICAL SEAMAP PLOTS
DAY 158 — 1422 DATA SPAN

4.3 MINI-RANGER RESIDUALS

When considering the results listed in Table 4.1, Table 4.2 and Figure 4.2, particular emphasis should be placed on the ranges designated Mini-Ranger #1. The transponder for this range link was mounted on the same tower as the C-Band transponder for the ship radar, providing essentially colinear range measurements. Thus the data could be compared without possible errors due to survey, geometry, or other measurements. The result yields a high degree of confidence in this range link. There is a definite possibility that the errors observed in the other range links (see also Figure 4.2) are due to a source such as survey errors, and that their error characteristics are actually similar to #1. If both Mini #2 and Mini #3 had approximately the same bias, there would have been reason to suspect an azimuth bias on the Wallops FPS-16. Since the biases were of opposite signs, an azimuth bias on the land radar seems unlikely. It is also possible that the errors observed were due to transponder antenna height or pointing. Motorola cautioned that transponder antenna pointing could be critical and excessive height could cause problems due to multipath. Furthermore, the Mini-Rangers were operating at the limit of their range.

Table 4.2. Mini-ranger Residual Statistics For Individual Data Spans

Data Span	Mini #1 (Meters) No. Data Points	Mini #1 (Meters) Mean	Mini #1 (Meters) Sigma	Mini #2 (Meters) No. Data Points	Mini #2 (Meters) Mean	Mini #2 (Meters) Sigma	Mini #3 (Meters) No. Data Points	Mini #3 (Meters) Mean	Mini #3 (Meters) Sigma
0030-0129Z	---	---	---	---	---	---	---	---	---
1422-1500Z	---	---	---	167	-5.8	3.4	82	-0.5	8.1
1612-1645Z	---	---	---	35	11.8	6.2	194	-5.2	4.6
1912-2000Z	53	-3.8	3.6	7	18.5	4.5	218	-6.2	4.9
2100-2200Z	---	---	---	---	---	---	---	---	---
1133-1212Z (June 7)	9	3.0	3.6	8	13.8	5.0	58	-6.3	4.4
OVERALL	62	-2.8	3.6	217	-1.5	4.4	552	-5.0	5.3

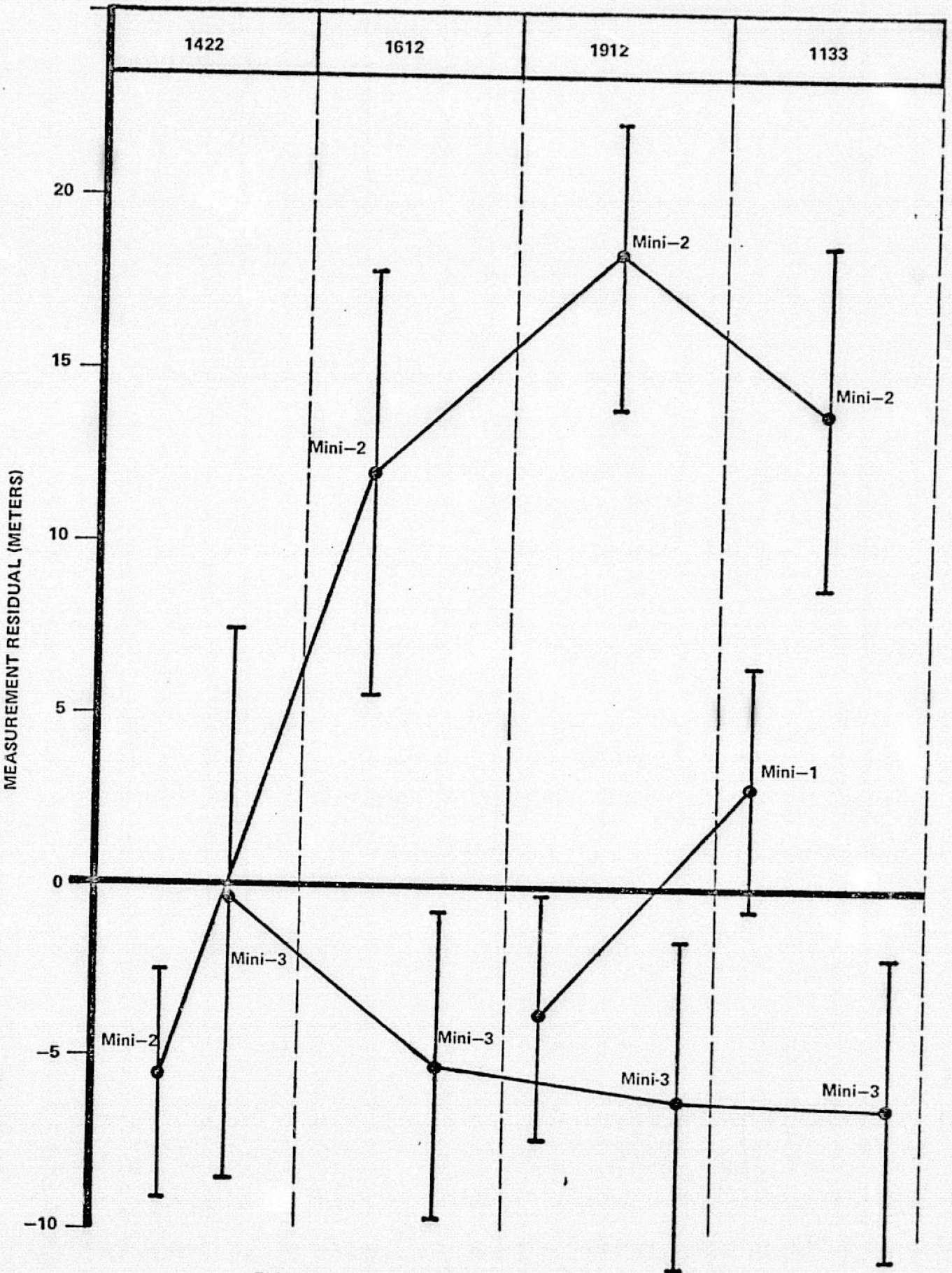

FIGURE 4.2. MINI–RANGER MEASUREMENT RESIDUALS
MEAN AND ONE SIGMA SPREAD

4.4 LORAN-C RESIDUALS

Figure 4.3 and Table 4.3 show the mean and one sigma spread of the LORAN-C residuals over all data spans. The 0030 span was eliminated from the Channel Y display (Figure 4.3) because of the large transients in this channel. From this plot, it is evident that the systematic errors in both channels did not change significantly between data spans.

The values listed in Table 4.3 include the secondary phase corrections and ASF corrections (see Appendix, Section 3.5). Therefore, the large Channel Z residual (-2581 m) is probably due to the receiver locking up on the wrong cycle. Since the carrier frequency is 100 KHz, one cycle is 10 μsec. In the MANSEE test area, 10 μsec delay from Channel Z represents 2431 meters. Had the receiver been properly locked, the true error would have been about 150 meters. Even this is larger than should be expected and may be due to an additional calibration error in the receiver since the results are quite consistent. It is also possible that the ASF correction (which accounts for propagation over land instead of seawater) was slightly in error. This was supplied by the U.S. Coast Guard and is computed as a "best fit" to measured data. For Channel Z, the slave station is located in Dana, Indiana, and the master station is in Carolina Beach, North Carolina. Thus, both the signal from the master to the slave and from the slave to the ship must travel over 1000 km of irregular terrain (Allegheny Mountains) which has varying conductivity. Furthermore, the path from the master to the ship is along the coast which also has varying conductivity. However, in spite of these problems, the error in the ASF correction should be less than 0.2 μsec or 49 meters.

The standard deviation of the Z-channel residuals is an order of magnitude larger than the Y residual sigma. This is a result of the frequent -200 m transients in the Z-channel which may also be related to improper receiver calibration.

Note the consistency of Channel Y (slave is on Nantucket Island). The mean residual only varied from -17 to -30 meters with 6 to 17 meters noise. For this channel, the scale factor in the MANSEE test area is 150 m/μsec. Thus, the -21 meter overall mean is an error of only 0.14 μsec.

Table 4.3. Loran-C Residual Statistics For Individual Data Spans

	Channel Y (Meters)			Channel Z (Meters)		
	No. Data Points	Mean	Sigma	No. Data Points	Mean	Sigma
0030-0130Z	---	---	---	348	-2570	181
1422-1500Z	179	-18	10	179	-2616	148
1612-1645Z	59*	-20	17	60	-2579	52
1846-1900Z	80	-30	9	80	-2565	58
1912-2000Z	96*	-17	6	97	-2580	58
2100-2200Z	191*	-21	14	192	-2575	71
1133-1212Z (June 7)	---	---	---	---	---	---
OVERALL	605	-21	12	956	-2581	133

*One bad Channel Y point was deleted

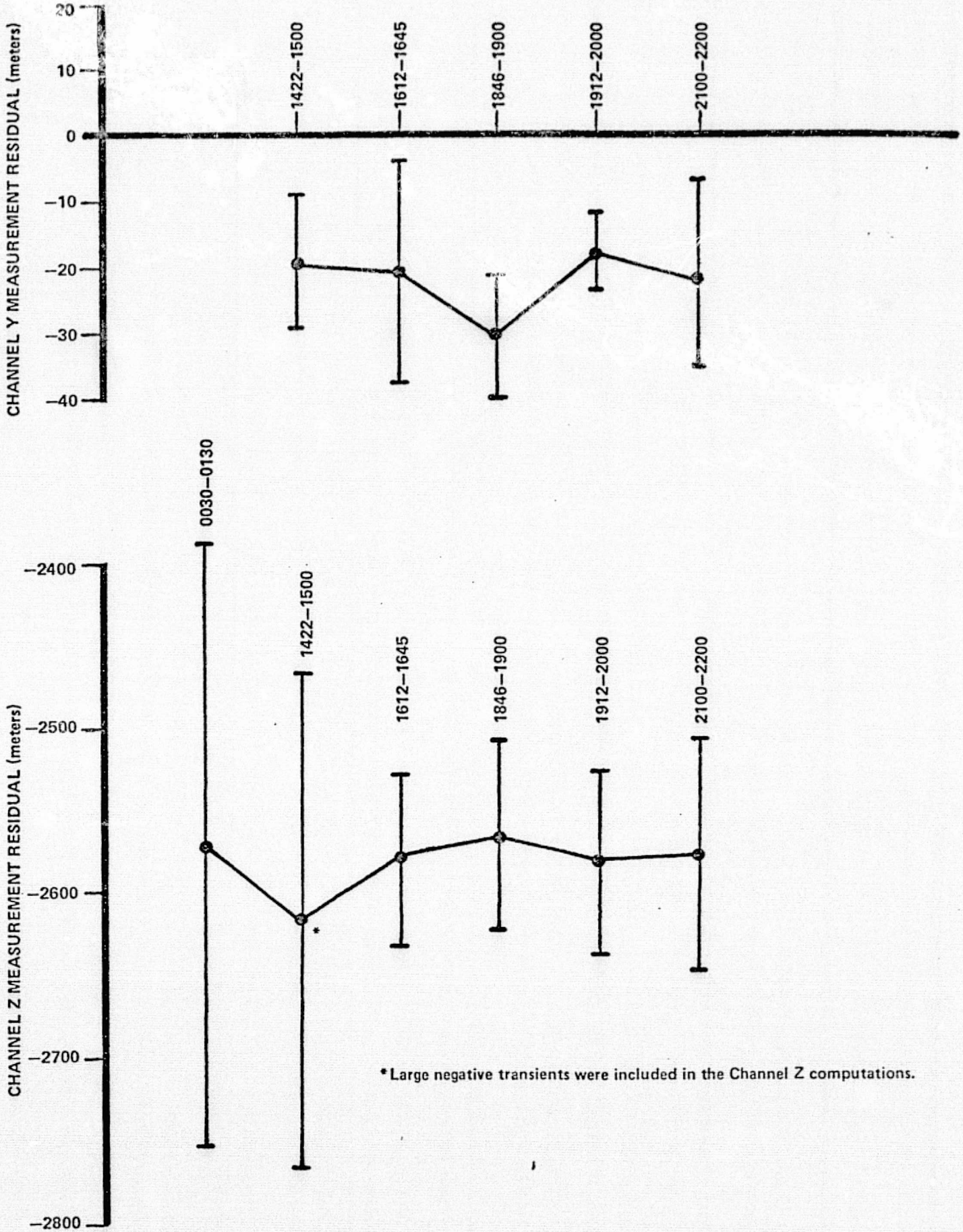

FIGURE 4.3. LORAN–C MEASUREMENT RESIDUALS
MEAN AND ONE SIGMA SPREAD

4.5 MK-19 RESIDUALS

From Table 4.1 the overall mean MK-19 heading residual is 3.3 degrees and the standard deviation is 2.3 degrees. From Table 4.4, the mean residuals for each data span varied from 2.1 degrees to 6 degrees and the corresponding standard deviations varied from 1.8 degrees to 3.6 degrees. When compared with the ground truth heading accuracy of $\pm$ 1 degree (one sigma), it can be concluded that the MK-19 heading measurements contained a positive bias. Since the MK-19 measures ship heading, while the ground truth computes the velocity vector, any ocean current would result in a bias between the two. However, the bias was fairly constant in all the data spans even though the ship changed headings. The residual plots showed no evidence of trending (Figure 4.4). Therefore, we can conclude that the residual standard deviations within each data span are good estimates of the measurement noise sigma.

Table 4.4. MK-19 Gyrocompass Heading Residual Statistics For Individual Data Spans

	HEADING DEGREES		
DATA SPAN	MEAN	SIGMA	NO. DATA POINTS
0030-0130Z	2.7	2.2	348
1422-1500Z	6.0	1.9	211
1612-1645Z	2.4	3.6	145
1912-2000Z	4.7	2.0	141
2100-2200Z	4.6	1.8	351
1133-1212Z (June 7)	2.1	2.8	225
OVERALL	3.3	2.3	1421

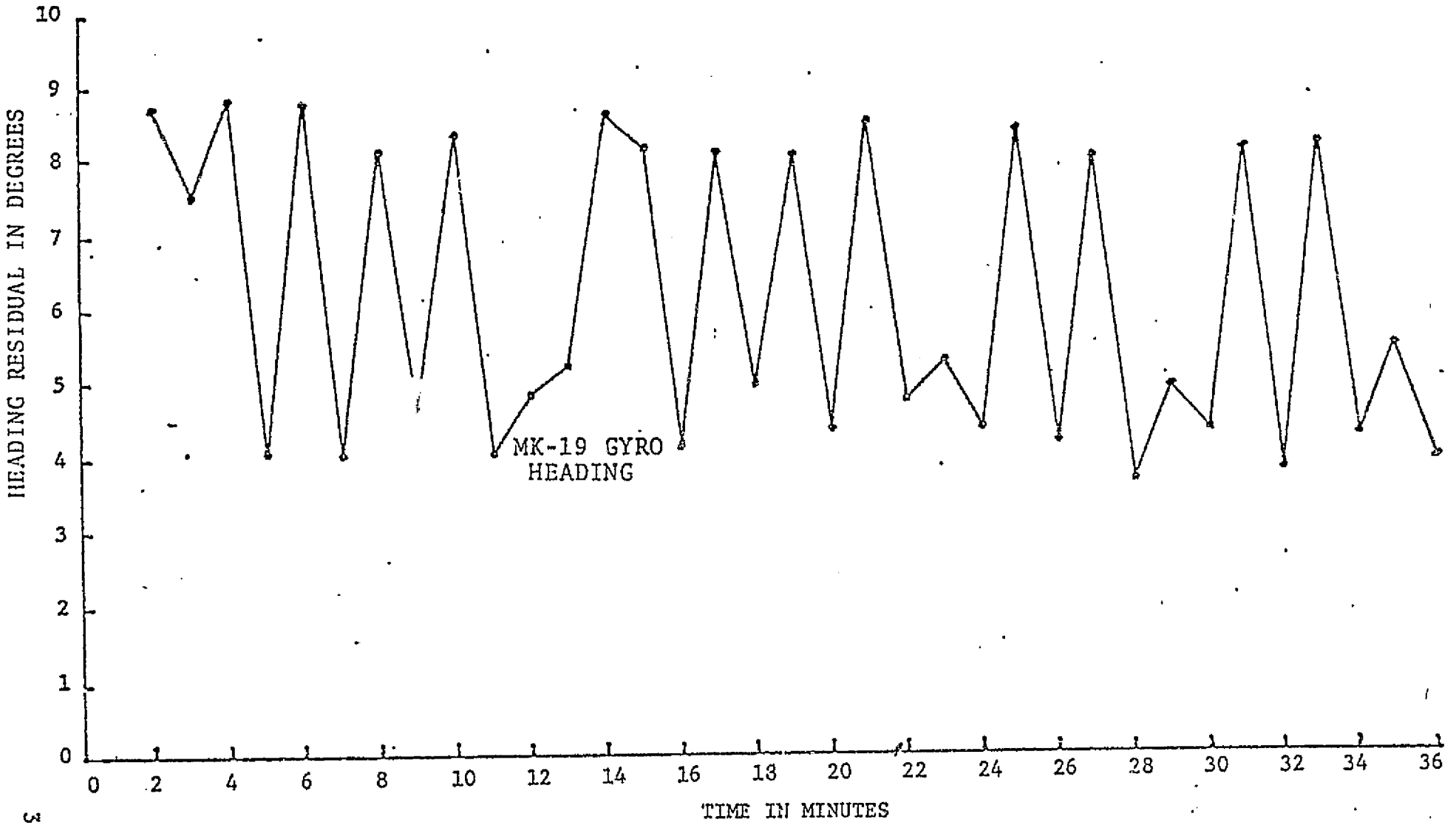

Figure 4.4. MARK-19 Heading Residuals, Day 158-1422 Data Span

4.6 AN/SRN-9 RESIDUALS

The AN/SRN-9 provided psoition fixes at approximately one hour intervals during the experiment. Unfortunately, June 6th was the only day on which simultaneous ground truth and AN/SRN-9 fixes were available. The mean and standard deviation of four position residuals are given in Table 4.1 and plots of residuals vs. time are given in Figure 4.5. The mean latitude residual is 100 meters and the standard deviation is 551 meters. The mean longitude residual of -170 meters can be attributed partly to the different geoids used within the AN/SRN-9 (NWL-8D) and within the SEAMAP Program (FISHER). This longitude difference on the North American continent is 51.4 meters at the MANSEE exercise latitude[1]. Thus, after adjusting for geoid differences, the actual mean longitude residual is 128.6 meters. Due to the limited number of data points, it is difficult to determine if the AN/SRN-9 errors are primarily random or systematic.

[1] Anderle and Smith, "NWL-8 Geodetic Parameters Based On Doppler Satellite Observations," NWL Report 2106, July 1967.

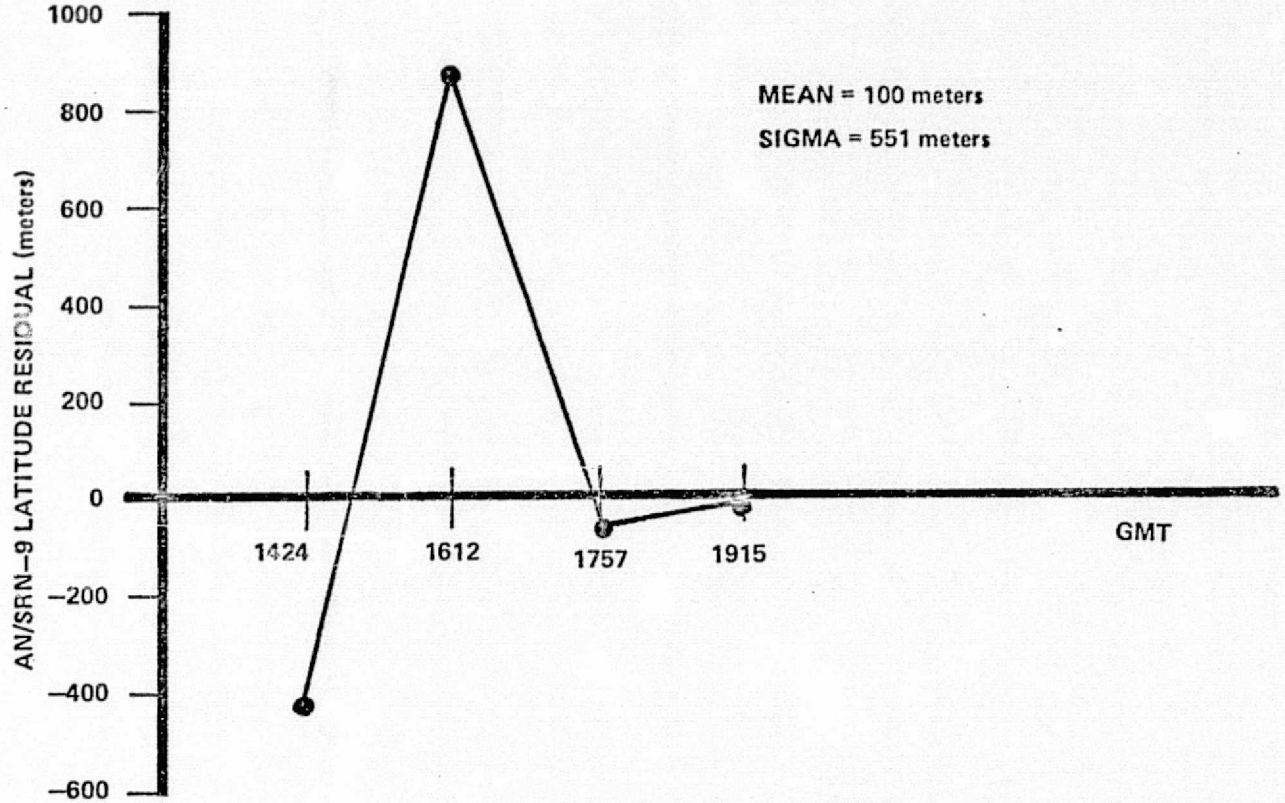

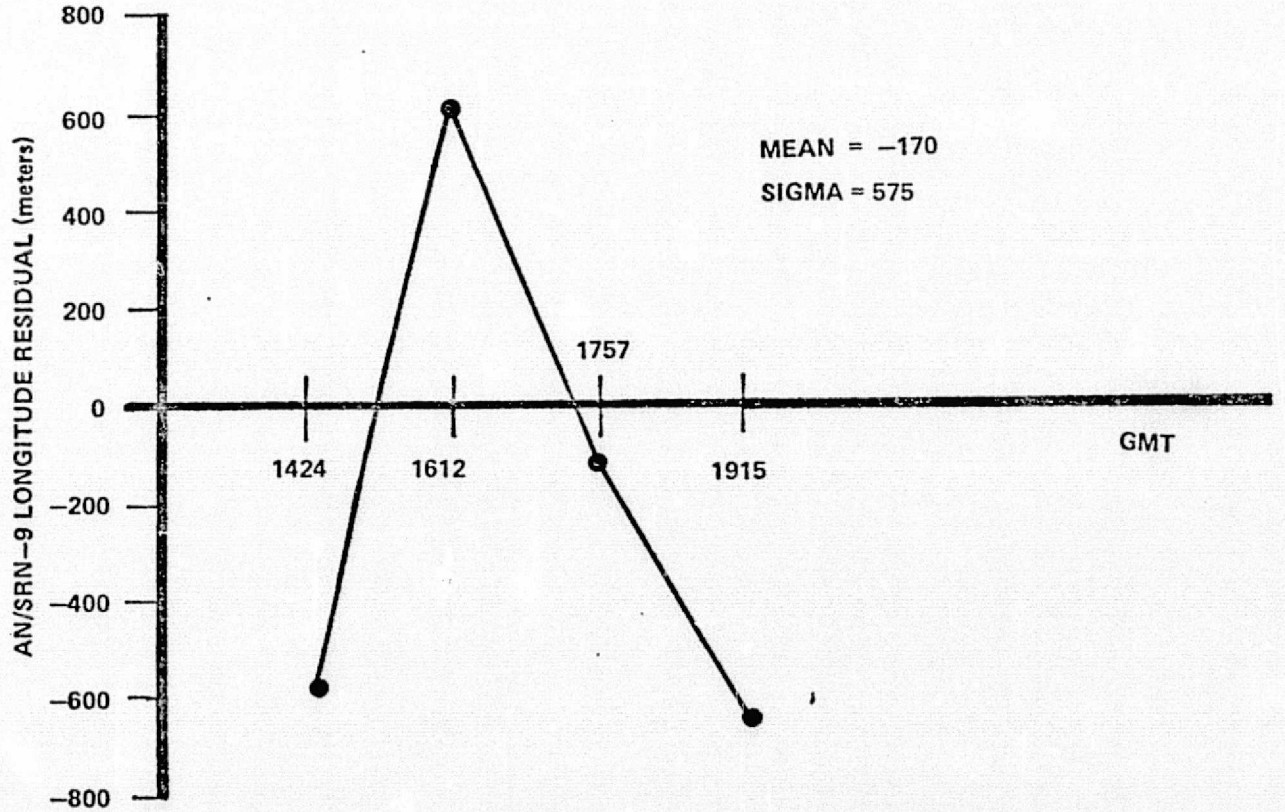

FIGURE 4.5. AN/SRN−9 POSITION RESIDUALS

4.7 OMEGA RESIDUALS

Table 4.5 lists the OMEGA residual statistics for all data spans and Figure 4.6 is a plot of the residuals. It is seen that the random error is generally smaller than the systematic component. The largest source of error is due to errors in the propagation correction. From the plots of the propagation correction versus time (see Appendix), it is seen that the correction changes drastically during the transition from night to day over the propagation path. Thus, the large errors during the 0030-0130Z and 1133-1212Z spans are due to errors in the rapidly changing propagation correction. However, it is interesting to note that the worst case errors are still within the stated accuracy of 1 nautical mile during the day and 2 nautical miles at night, despite the fact that the ship is only 350 nautical miles from station D (Forrestport, New York).*

*The propagation corrections are somewhat less accurate for ranges less than 450 nautical miles.

Table 4.5. Omega Residual Statistics For Individual Data Spans (Including Propagation Corrections)

Data Span	Stations B-C			Stations D-F		
	No. Data Points	Mean	Sigma	No. Data Points	Mean	Sigma
0030-0130Z*	23	-117	746	23	3067	946
1422-1500Z	16	-557	997	16	-696	99
1612-1645Z	10	736	339	10	-309	176
1846-1900Z*	6	-1287	109	6	-1085	120
1912-2000Z	11	-1457	156	11	-1298	114
2100-2200Z	25	-1459	308	25	-295	209
1133-1212Z	16	-2926	207	16	-9	344
OVERALL	107	-1040	611	107	262	589

*Ground truth is in error by about 50 meters.

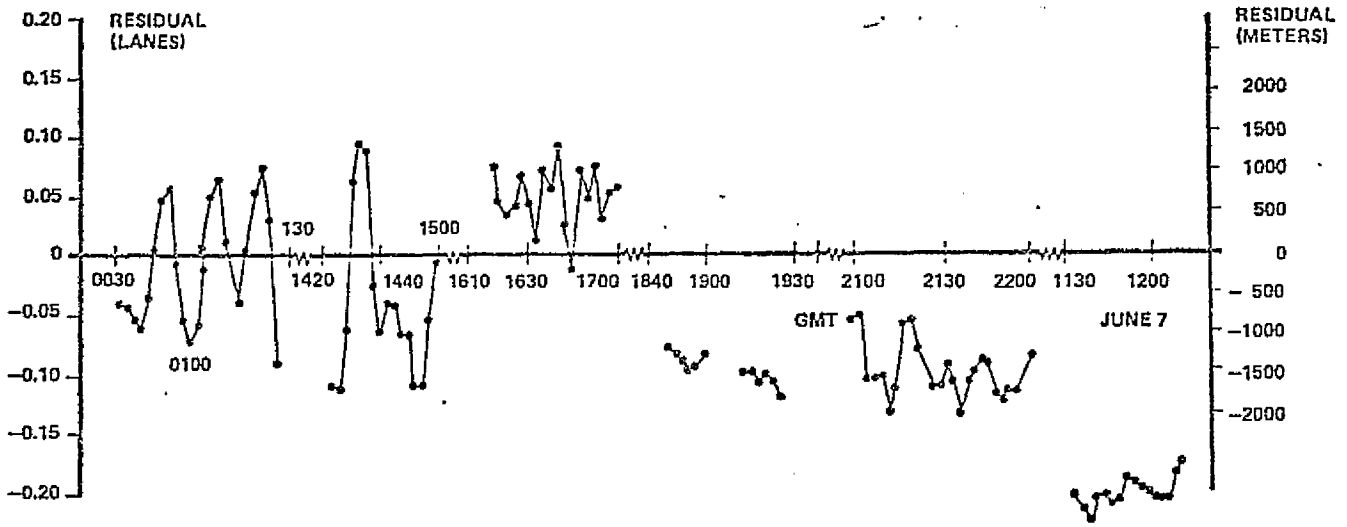

OMEGA RESIDUALS FOR STATIONS B–C
(TRINIDAD – HAWAII)

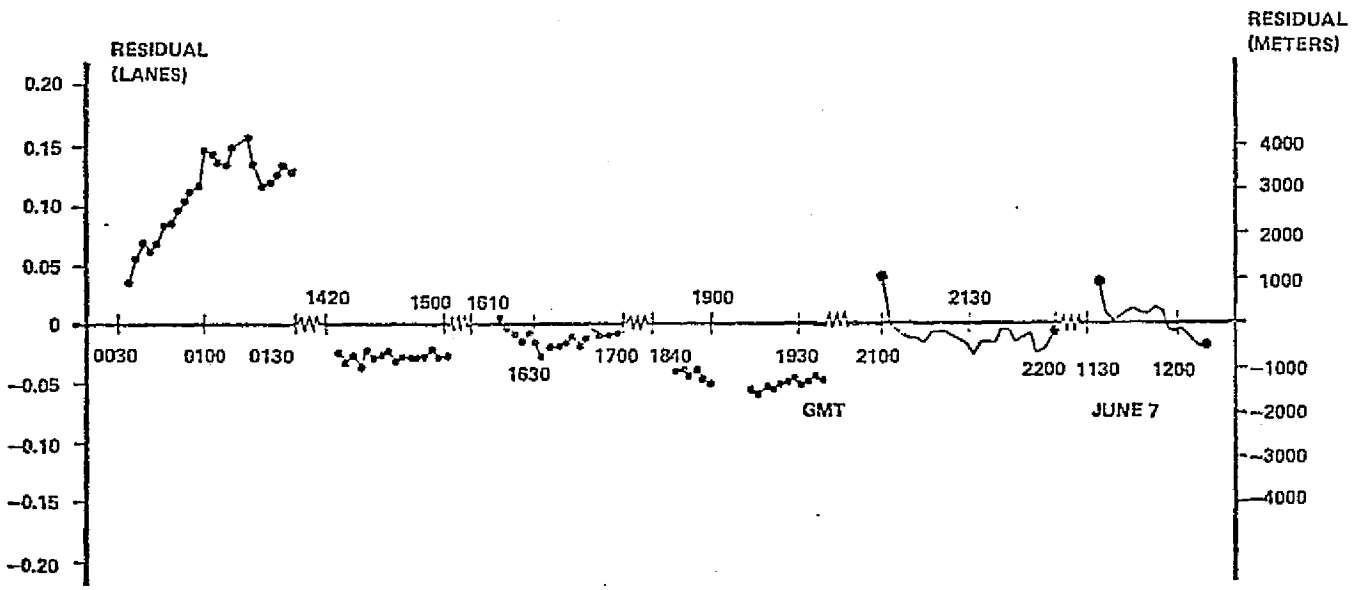

OMEGA RESIDUALS FOR STATIONS D–F
(NEW YORK – NORTH DAKOTA)

FIGURE 4.6. OMEGA RESIDUALS

4.8 RAYDIST-T RESIDUALS

Table 4.6 and Figure 4.7 show the mean and one sigma spread of the Raydist residuals. Considering that the MANSEE test area was outside the prime coverage area of the Raydist network (see Figure 4.8), the random Raydist residuals are quite small (Approximately 0.03 lanes). Since the ground truth, RMS position error due to measurement noise (radars) and state noise is about 3 meters, it cannot be stated whether the Raydist residuals are due to errors in the ground truth or to Raydist error. The nominal accuracy of the Raydist network is 0.02 lanes which is about 2 meters in the MANSEE test area.*

The spread of the mean residuals was 8.7 to 34.2 meters for the Red Channel and -1.8 to -16.7 meters for the Green Channel. The spread of the means is far more meaningful than the actual values of the means since the Raydist receiver was not accurately initialized during the test. Thus the overall means of 23.8 meters (Red Channel) and -11.1 (Green Channel) are simply indications of the initialization error. The spread of the means is somewhat larger than expected. In particular, the 8.7 meter Red Channel mean for the 1612 data span and the -16.7 Green Channel mean for the 1422 data span stand out. Both of these mean residuals are difficult to explain. For the 1612 data span, the Red Channel measurement is indicating that the ship should be about 16 meters northwest of the ground truth position. This is the only data span in which the Wallops FPS-16 range did not agree with the Vanguard FPS-16 range. However, if the Wallops radar is correct, the actual ship position is 8 meters southeast of the ground truth position.

*In the MANSEE test area, one lane is 112.0 and 82.1 meters respectively for the Red and Green Channels.

Likewise, in the 1422 data span, the Raydist Green Channel indicates that the ship is about 10 meters north of the ground truth position. Miniranger #2 tends to confirm this, but the accuracy of the Minirangers is not sufficient to state a definite conclusion.

During the MANSEE exercise, the Raydist receiver temporarily lost track on two occasions and had to be reset manually by examining strip chart recordings. The first time was on the evening of June 5 and the second was early morning on June 7. Thus the manual resetting could not explain the spread of the mean Raydist residuals. There was also a period after 1400Z on June 6 when the Days Point station (Green Channel) was transmitting at low power. This might explain the discrepancy in the Green Channel mean for the 1422 data span. Apparently the receiver lost track between 1422Z and 1612Z because both channels have a +1 lane offset between the 1422 data spans and the other data spans. Likewise, there was a -1 lane, Green Channel offset in the 2100Z data span.

Table 4.6. Raydist Residual Statistics For Individual Data Spans

Data Span	Red Channel			Green Channel		
	No. Data Points	Mean	Sigma	No. Data Points	Mean	Sigma
1422-1500Z	729	24.2	3.0	728	-16.7	2.5
1612-1645Z	253	8.7	3.0	253	-7.8	5.6
1912-2000Z	235	28.9	1.7	235	-1.8	3.1
2100-2200Z	200	24.0	1.5	200	-6.7	2.0
1133-1158Z	215	34.2	4.1	215	-10.3	4.3
OVERALL	1632	23.8	2.9	1631	-11.1	3.5

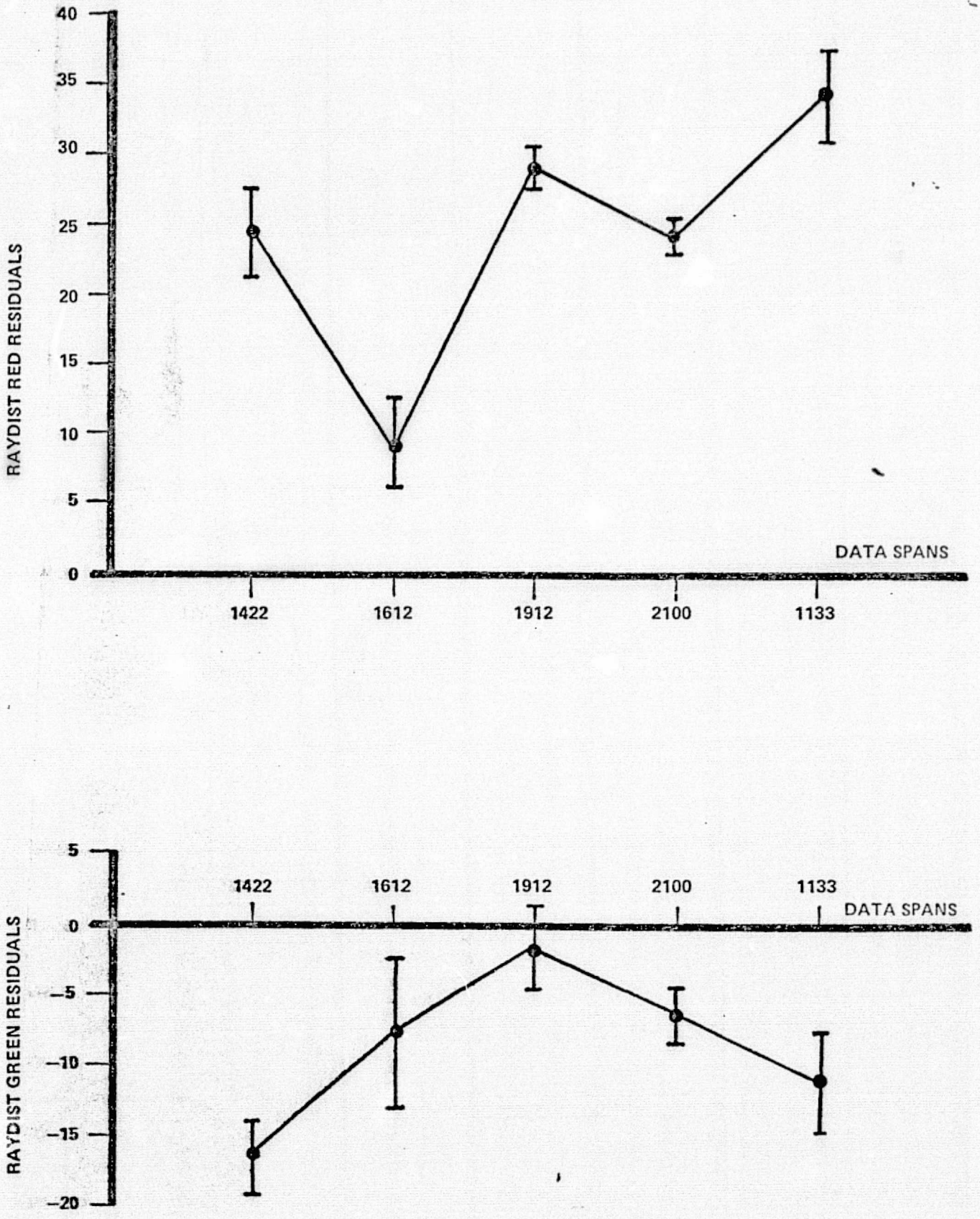

FIGURE 4.7. RAYDIST MEASUREMENT RESIDUALS
MEAN AND ONE SIGMA SPREAD

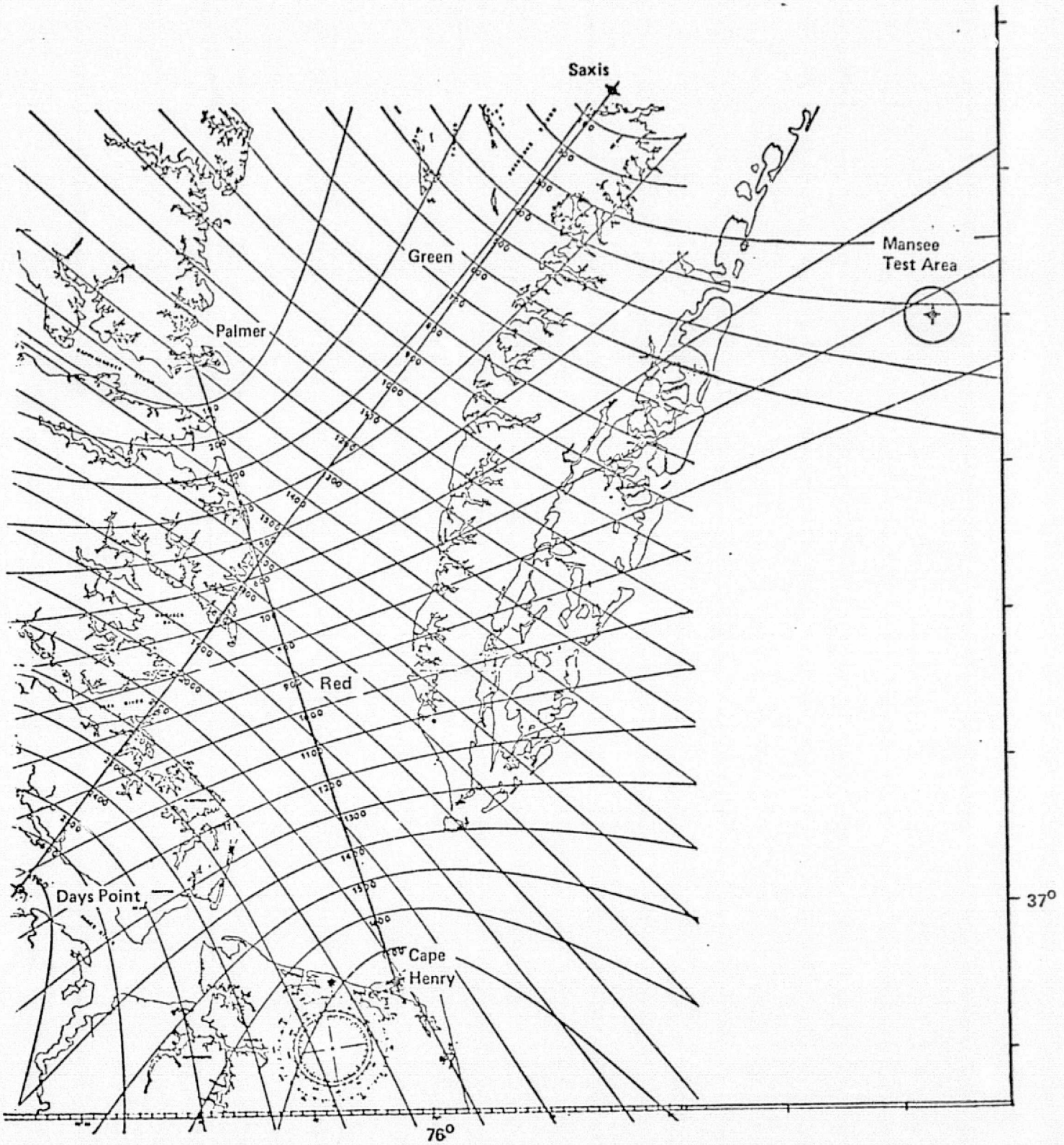

FIGURE 4.8. RAYDIST NETWORK

LOWER CHESAPEAKE BAY COVERAGE, HYPERBOLIC GEOMETRY

SECTION 5.0
NAVIGATION FILTER RESULTS

The previous section gives detailed measurement error characteristics for individual sensors. This section summarizes the overall navigation accuracy achievable with various sensors and combinations of sensors. Here the sequential filter in SEAMAP was used to process a time sequence of navigation measurements and to give a current estimate of ship position (Φ,λ) and velocity ($\dot{x},\dot{y}$). Error analysis computations within the program converted sensor measurement error statistics into predicted navigation error levels (RMS position error, RMS velocity error). The actual navigation errors (RSS position error, RSS velocity error) were evaluated by differencing the estimated trajectory with the corresponding ground truth trajectory.

5.1 COMPARISON OF ACTUAL AND PREDICTED NAVIGATION ERRORS

Figures 5.1, 5.2 and 5.3 show comparisons of actual position errors (RSS) and predicted error levels (RMS). In filtering the Mini-Ranger data (Figures 5.1 and 5.2), the RMS error was of the same magnitude as the RSS error when two Mini-Rangers were tracking and their error characteristics were correctly modeled. The RMS error was computed assuming 4 meters random noise, 3 meters bias, 4 meters latitude error and 3.2 meters longitude error. In Figure 5.1, the RSS error was more than double the RMS error during the period from 1442 to 1449Z. During this period, the tracking from Mini-Ranger #3 became intermittent and its error characteristics suddenly changed (see Figure 4.1). The bias appeared to change by almost 10 meters after 1442Z. Likewise in Figure 5.2, the RSS error suddenly grew when Mini-Ranger #1 dropped out and Mini-Ranger #2 began tracking. Mini-Ranger #2 had a bias of +19 meters for this span (Table 4.2).

In filtering the Loran-C data, all propagation corrections were applied to the data and the one cycle (10 microseconds) error in the Z channel was corrected so that the results more realistically model actual Loran performance. Figure 5.3 shows the comparison of RSS and RMS position errors assuming 1 μsec random noise and 0.2 μsec phase correction error for each channel (other error sources were negligible). The RSS errors ranged from 104 to 207 meters and during most of the span, they were approximately 50% greater than the predicted (RMS) error. The major source of error is the 150 meter, uncorrected bias in the Z channel. As discussed in Section 4.4, this represents about 0.6 μsec error which is three times larger than the propagation error assumed in computing the RMS position error. Hence, the discrepancy between RMS and RSS errors is expected.

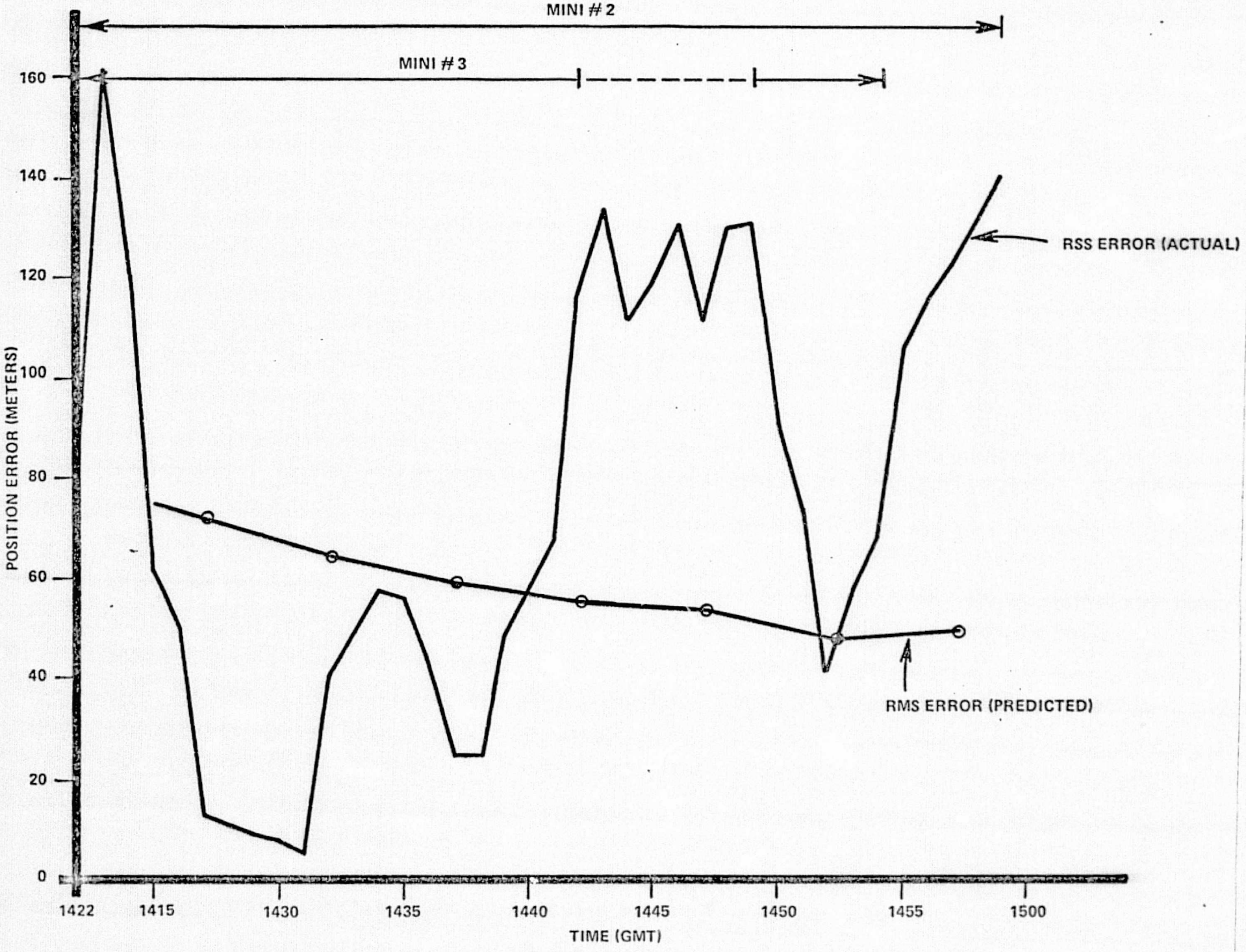

FIGURE 5.1. MINI-RANGER FILTER RMS AND RSS POSITION ERRORS – 1422 DATA SPAN

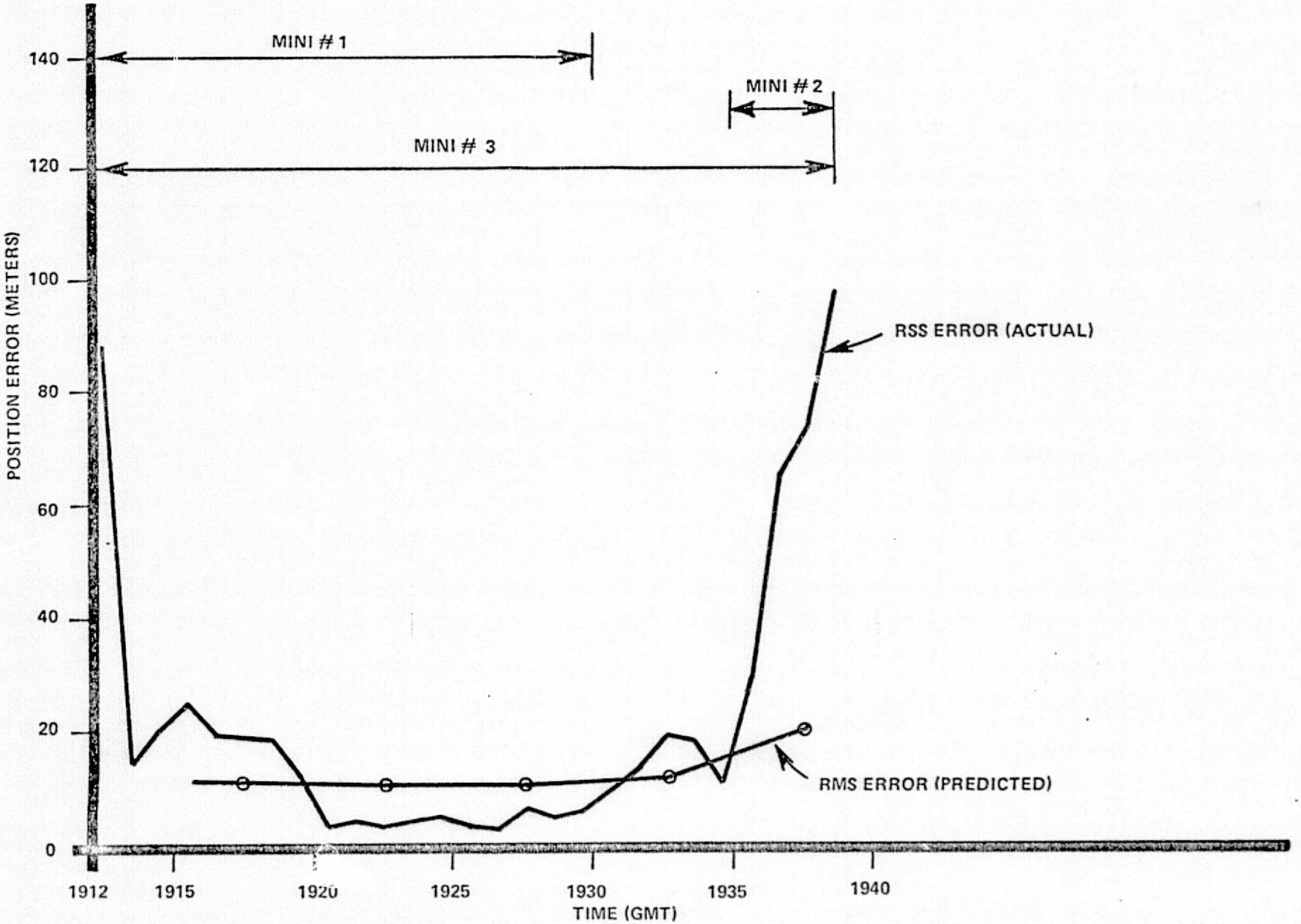

FIGURE 5.2. MINI-RANGER FILTER RMS AND RSS POSITION ERRORS – 1912 DATA SPAN

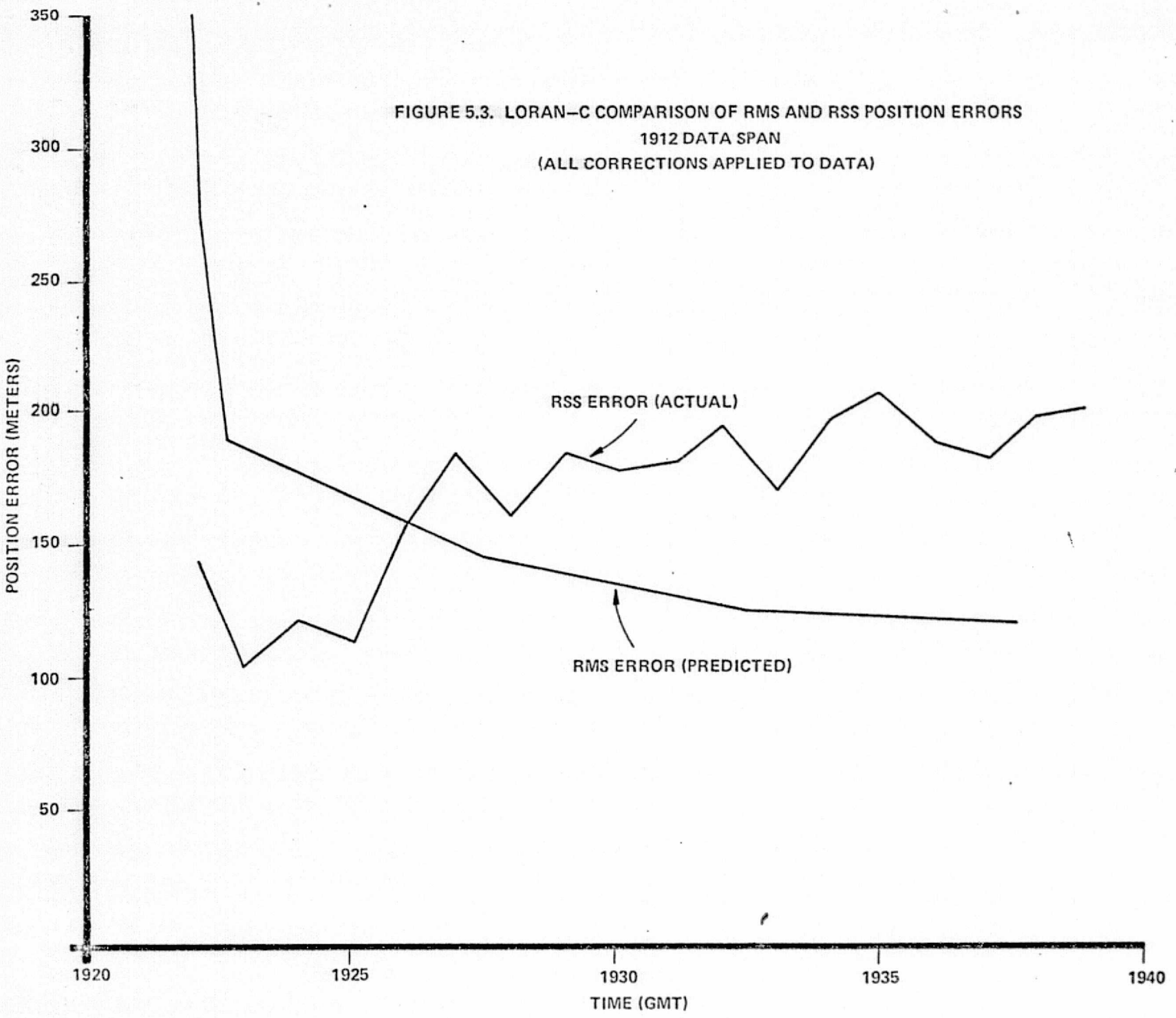

FIGURE 5.3. LORAN–C COMPARISON OF RMS AND RSS POSITION ERRORS
1912 DATA SPAN
(ALL CORRECTIONS APPLIED TO DATA)

5.2 COMBINATION OF VELOCITY DATA WITH LORAN-C POSITION DATA

Figures 5.4, 5.5 and 5.6 show the effect of using the SEAMAP filter to combine the Loran position data with velocity data accurate to 0.1 m/sec. These results represent an upper bound on the navigation accuracy improvement derived from combining velocity data with Loran-C position data.

The 1618 data span (Figure 5.4) is somewhat unusual in that the RSS error when using velocity data is greater than with Loran data only. The second Loran-C, Z channel, data point in this span was in error by 10 μsec (2431 m). Since this occurred at the very beginning of the run when the data editor was turned off,* the position estimate was grossly in error. As additional Loran data was processed, the position estimate returned close to the correct position. However, the inclusion of velocity data made the filter overconfident in its estimate and the filter gain matrix became far too small. Thus new Loran position fixes were essentially ignored.

Figures 5.5 and 5.6 are more typical of the improvement expected when velocity data is added to Loran position fixes. The improvement is not great because the dominant error is the 150 meter bias in the Z channel of Loran. In fact, Figure 5.6 shows that the RSS error, when using velocity data, can exceed the Loran only error for a considerable period of time. This is again due to the reduction in the filter gain matrix when the additional measurement type is added.

*The data editor is inoperative for the first 100 seconds of the run so that initialization errors do not result in the rejection of good data.

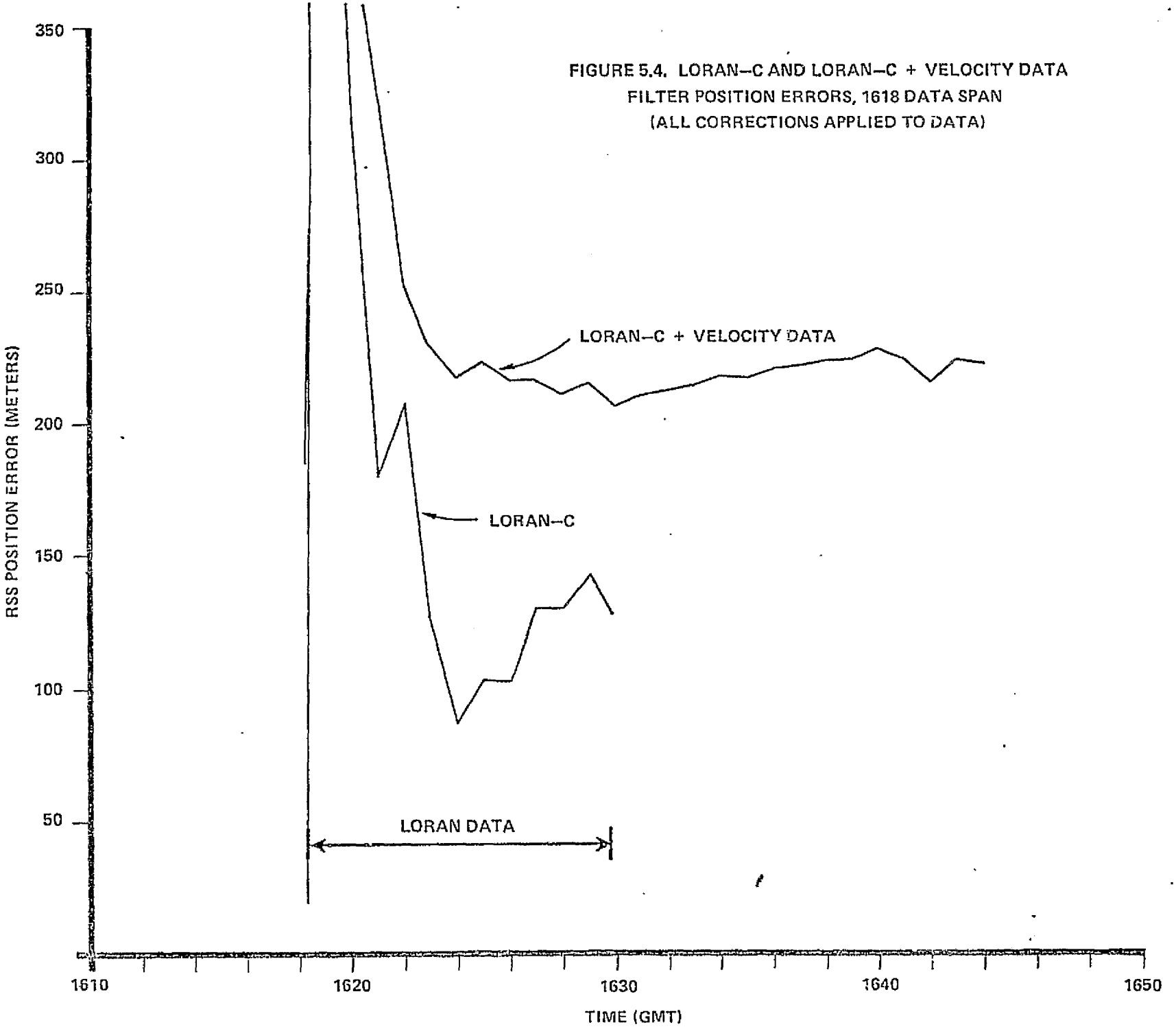

FIGURE 5.4. LORAN–C AND LORAN–C + VELOCITY DATA FILTER POSITION ERRORS, 1618 DATA SPAN (ALL CORRECTIONS APPLIED TO DATA)

FIGURE 5.5. LORAN–C AND LORAN–C + VELOCITY DATA
FILTER POSITION ERRORS, 1912 DATA SPAN
(ALL CORRECTIONS APPLIED TO DATA)

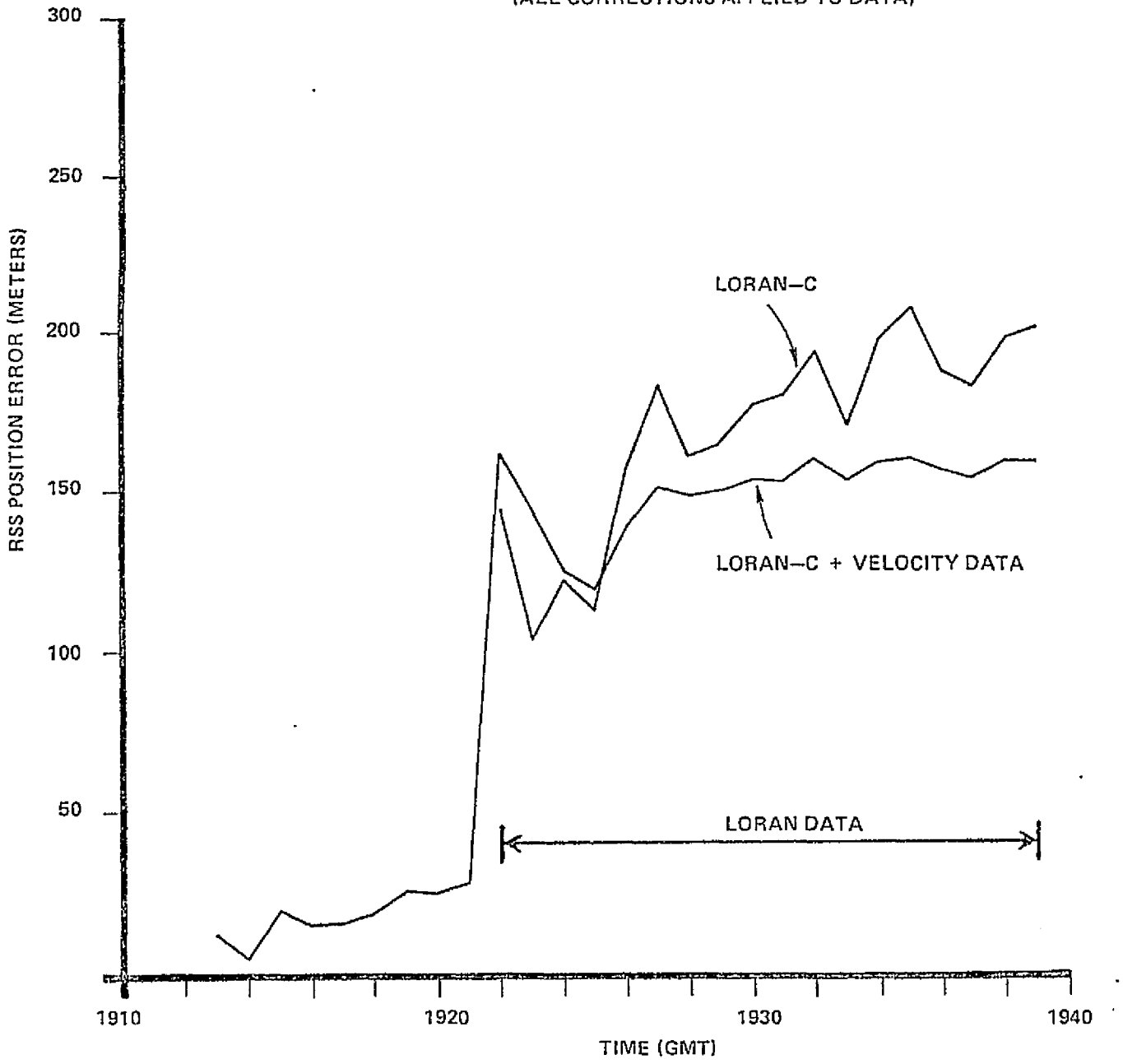

FIGURE 5.6. LORAN–C AND LORAN–C + VELOCITY DATA
FILTER POSITION ERRORS, 2100 DATA SPAN
(ALL CORRECTIONS APPLIED TO DATA)

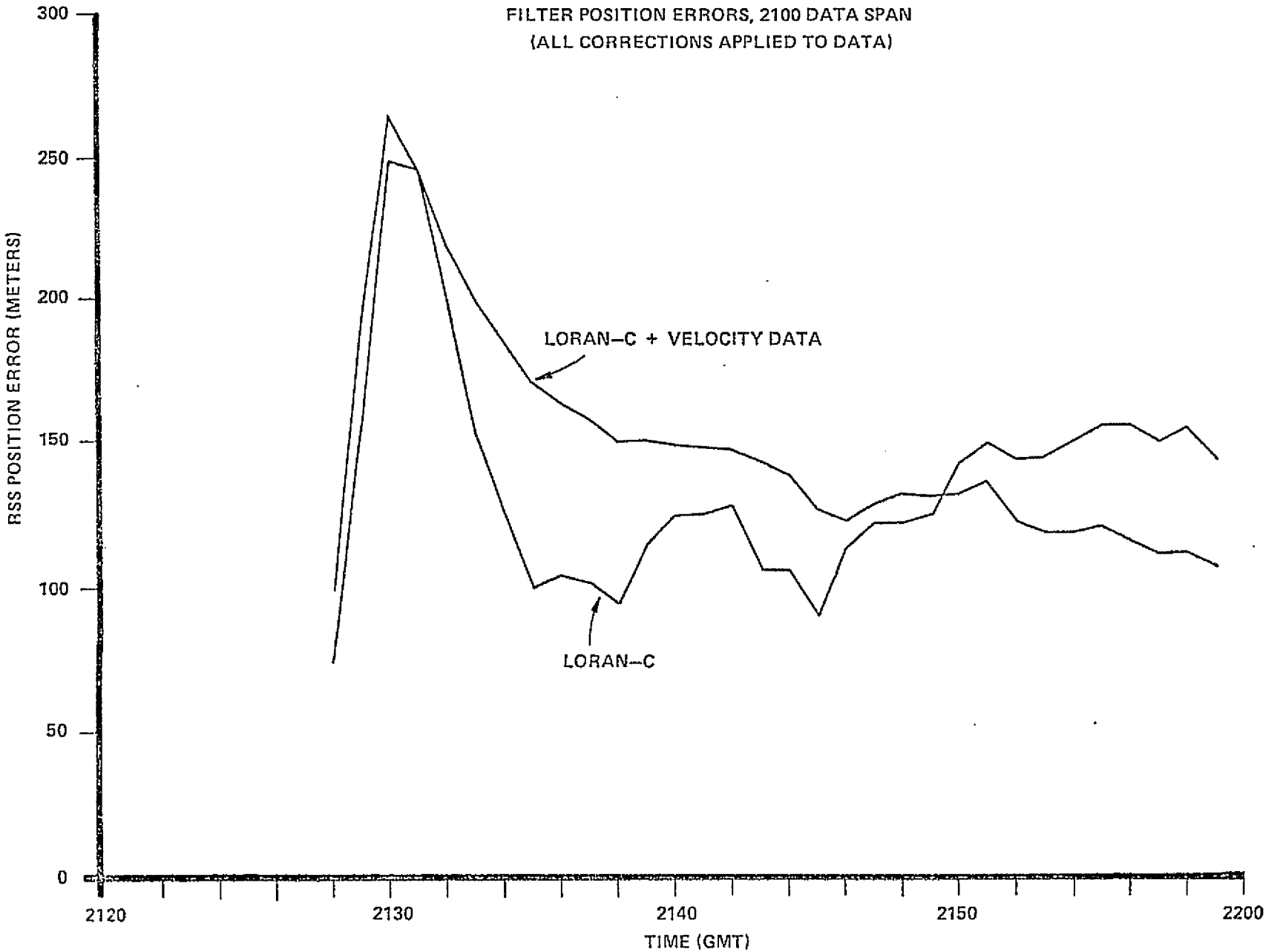

5.3 DATA EDITING EXAMPLE

SEAMAP contains a statistical data editor which compares each measurement residual vector with its analytically computed covariance matrix. Outlying components of the residual are deleted prior to processing by the sequential filter. During the 1612 data span an equipment malfunction in the LORAN receiver introduced a -100 μsec (-15,000 m) bias in the Channel Y data (see Figure 5.7). This data transient caused the filter position estimate to be in error by 20,000 meters. With the data editor activated, all of the bad Channel Y data was deleted and the filter solution, using only Channel Z data, showed no noticeable deterioration during the twenty minutes following the initial transient. The inclusion of velocity data would have allowed the filter to follow reasonable changes in ship velocity during this period of bad LORAN data.

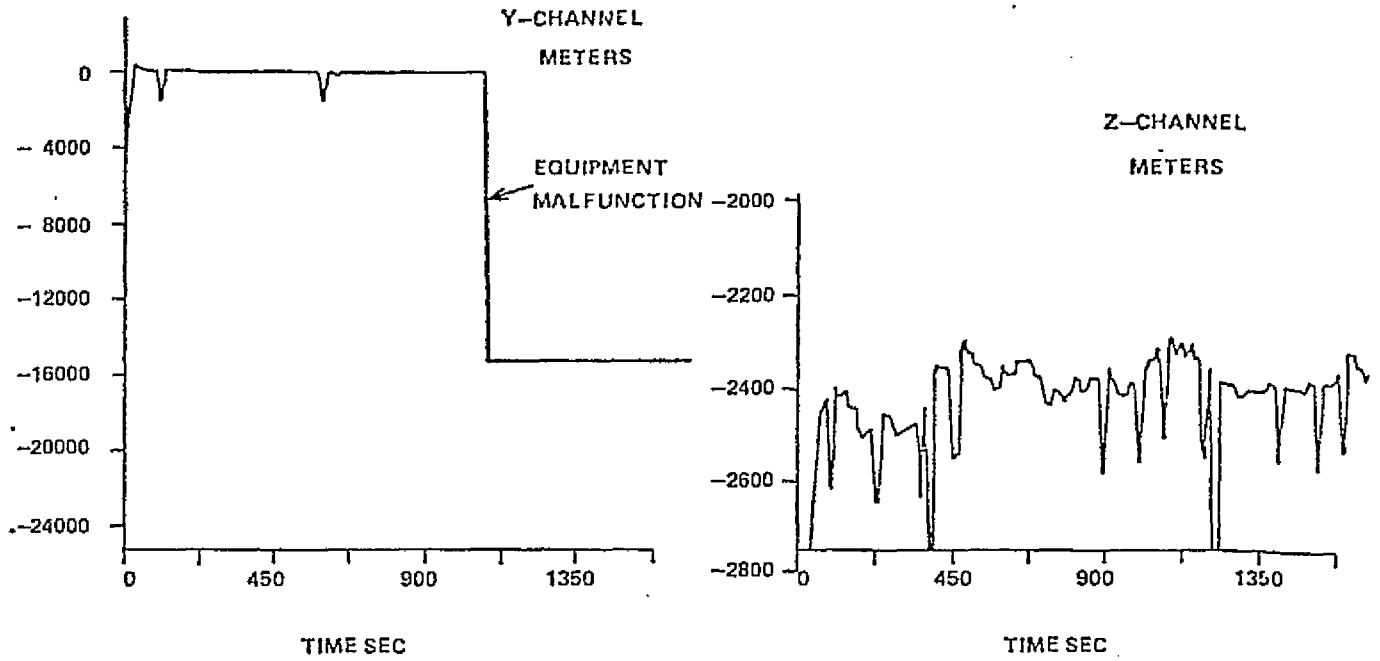

LORAN–C RESIDUALS FROM GROUND TRUTH PROCESSING

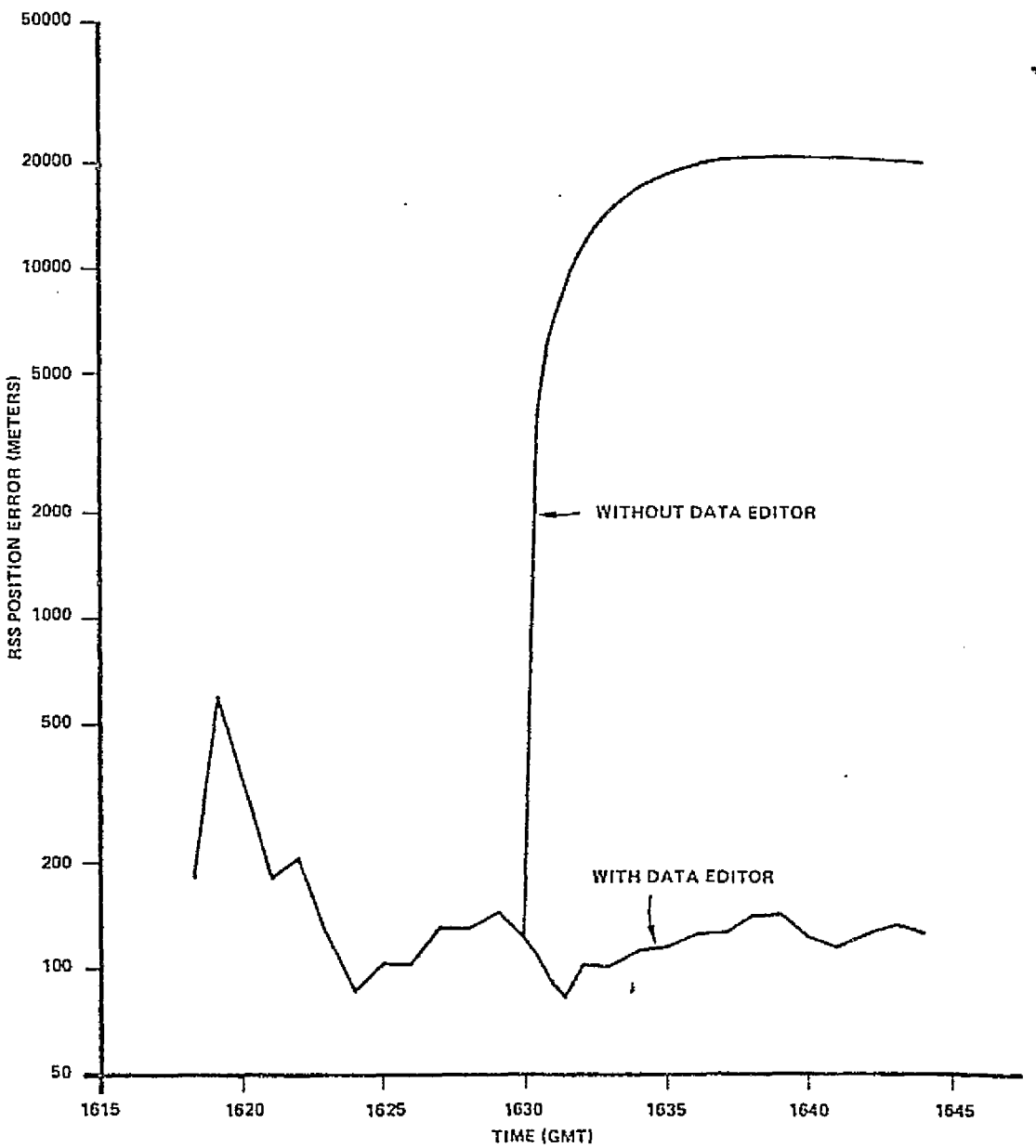

FIGURE 5.7. PROCESSING OF LORAN–C 1612 TIME SPAN SHOWING EFFECT OF DATA EDITOR

SECTION 6.0
CONCLUSIONS

In performing the MANSEE experiment and subsequent data analysis, NASA/Wallops station has demonstrated the test planning, instrumentation, and data processing capability to utilize multiple sensors in establishing a ground truth ship trajectory accurate to $\pm$ 5 meters (one sigma). This value is considered to be a "worst case" one sigma, as the survey uncertainty of six meters used in the error propagation is a pessimistic value. The accuracy was achieved by using a generalized sequential filter (SEAMAP) to process combined data from the two C-Band tracking radars. The availability of higher data rates with the Wallops radars indicates the potential for obtaining the same or better accuracy for numerous other navigation and traffic control testing applications, particularly in aeronautics.

Following the experiment, data analysis with the SEAMAP program demonstrated the desirability of redundant ground truth instrumentation. Comparison of azimuth residuals with pre and post-mission calibration data showed that the ship radar azimuth measurements contained systematic errors two orders of magnitude greater than those for the land based radar. Elimination of ship azimuth measurements reduced ground truth position errors from 10-20 meters RMS to 5 meters RMS.

The usefulness of a sequential filter in processing measurements subject to intermittent data losses or transients was demonstrated. In the case of LORAN-C, SEAMAP successfully processed through 20 minutes of bad Channel Y data while providing an adequate navigation solution.

The scope of this effort did not include an indepth analysis of all data from all sensors, but rather attempted to indicate the overall characteristics of each. Thus, the results presented here only summarize the operational error characteristics of the particular navigation instrumentation installed on the VANGUARD during the MANSEE test.

Most of the navigation sensors performed as expected. The only exceptions were the Z channel of Loran-C (which apparently locked up on the wrong cycle of the carrier) and the AN/SRN-9 (which had only 4 data points). To summarize, a comparison of the overall RSS residuals obtained from ground truth processing with the nominal accuracy of the systems is given below:

	Nominal Accuracy	RSS Residual
Mini-Rangers	3 m	6.5 m
Loran-C	15-400 m	2023 m
MK-19 GYRO	?	4.0°
AN/SRN-9	100-370 m	580 m
Omega	1852 m	967 m
Raydist-T	2 m	3.2 m*

In the case of the Mini-Rangers and Raydist-T, the RSS residual cannot be interpreted as the true error because of 5 meter uncertainty in the ground truth.

*Does not include mean error which is due to improper initialization.

APPENDIX
SEAMAP
MATHEMATICAL DESCRIPTION

March 1975

Prepared For

NASA/Wallops
Wallops Flight Center
Wallops Island, Virginia 23337

Prepared By

William Hatch
Bruce Gibbs

Wolf Research and Development Group
EG&G/Washington Analytical Services Center, Inc.
6801 Kenilworth Avenue
Riverdale, Maryland 20840

Planetary Sciences Department Report No. 007-75

SECTION 1.0
INTRODUCTION

The "SEAMAP" program is designed to process multi-sensor maritime navigation data to obtain an optimal estimate of ship position (ϕ,λ) and velocity $(\dot{x},\dot{y})$. The program has extensive error analysis capability for optimal or sub-optimal treatment of sensor static error parameters such as measurement bias and station location errors.

This report contains a mathematical description of the sequential filter, sensor models and state dynamic model contained in "SEAMAP."

Figure 1.1 shows overall structure of a sequential filtering program which processes an ordered time sequence of measurements $\{y_1, y_2 \ldots y_n \ldots\}$. The state dynamic model computes the state and the transition matrix at time t_n given the state at t_{n-1}. From this state the sensor models compute the a priori or anticipated measurement and the partial derivatives of this measurement with respect to the state. The filter combines these quantities with the actual measurement to obtain an updated or aposteriori estimate of system state.

In "SEAMAP" the filter, dynamic model and each sensor model have been programmed as independent software modules such that any one can be modified or replaced without disturbing the remaining code.

SECTION 2.0
SEQUENTIAL FILTER DESCRIPTION

If navigation filter accuracy is predicted under the assumption that sensor errors are entirely due to zero mean random noise previous WOLF studies (2) have indicated that the presence of additional static errors, such as sensor bias, can result in considerable deviation of the actual filter accuracy from the predicted values. In many cases these static parameters are not observable and therefore cannot be included in the state vector of adjusted parameters. Johnson (1) has derived a generalized linear filter which considers a priori knowledge of these unobservable parameters in computing an optimal sequence of filter weight matrices.

These previous developments have been incorporated by WOLF into the design of SEAMAP.

SEAMAP contains a generalized linear filter which processes multisensor marine navigation data. The filter has extensive capability for treating static error parameters in the sensor models (such as measurement bias and station location errors). Each static error parameter may be treated by the filter as:

- Adjusted - the static parameter is included in the state vector of parameters to be adjusted.

- Consider - a considerable parameter is not adjusted but its uncertainty is taken into account where computing the filter weighting matrices. This means that the filter is able to make optimal use of any a priori knowledge about the uncertainty in parameters which are unobservable.

- Analyze Only - error analysis computations external to the filter compute the additional uncertainty in each adjusted parameter due to the uncertainty in each analyze only parameter. The display of these uncertainties (one sigma) gives the detailed numerical consequences of omitting a parameter from the filtering computations.

Classification of each static parameter is designated by card input for any given filter run.

Outlying data points may cause the filter to diverge or go out of control. SEAMAP contains statistical data editing logic which deletes outlying measurements.

The following sections describe the generalized linear filter equations implemented in SEAMAP. In these discussions and flow charts the subscripts of each of the vectors or matrices refer to first the data point at which the matrix or vector is being evaluated, and second, the data point at which observation data was last incorporated into the estimate. Thus $\underline{X}_{i/i-1}$ means the estimate prediction of $\underline{X}$ at data point i, based on observation data through data point i-1. $\underline{X}_{i-1/i-1}$ means the estimate of $\underline{X}$ at data point i-1, based on observation data through data point i-1. $\Phi_{i,i-1}$ is evaluated at $X_{i-1} = X_{i-1/i-1}$.

2.1 STATE AND MEASUREMENT MODELS

The state vector can be partitioned as:

$$\underline{X}_n = (\underline{X}_n^d, \underline{X}_n^1, \underline{X}_n^2 \ldots \underline{X}_n^\ell)$$

where:

$\underline{X}_n^d$ = dynamic force model terms such as position and velocity which must always be included in the set of adjusted parameters.

$\underline{X}_n^1$ = adjusted and consider parameters such as measurement bias and station location errors for sensor number one.

$\underline{X}_n^2$ = same for sensor number two.

$\vdots$

$\underline{X}_n^\ell$ = same for sensor number ℓ.

The elements of $\underline{X}_n^d$ must always be adjusted while the adjustment of any static error parameter is optional.

It is assumed that the incremented state model has the form:

$$\underline{X}_n^d = \underline{f}_n \left(\underline{X}_{n\ n-1}^d\right) + \underline{q}_n$$

where $\underline{q}$ is a zero mean vector of state noise having covariance matrix Q_n.

A measurement from the k^{th} sensor is related to the current state by:

$$y_i^k = \underline{m}_i^k \left(\underline{X}_i^d, \underline{X}_i^k, \underline{s}^k\right) + \underline{r}_{i_k}^k$$

where $\underline{r}_i^k$ is a zero mean noise vector having covariance matrix R_i^k and $\underline{s}^k$ contains those static error parameters of the k^{th} sensor which are treated as unadjusted analyze.

2.2 FILTER EQUATIONS

For a typical filter cycle it is assumed that a priori errors in the adjusted parameters can be approximated by a linear combination of four statistically independent error vectors.

$$\delta\underline{X}_{n/n-1} = L_{n/n-1}\underline{s} + W_{n/n-1}\delta\underline{X}_{o/o} + \underline{b}_{n/n-1} + \underline{g}_{n/n-1}$$

where:

$L_{n/n-1}\underline{s}$ = component due to errors in unmodeled analyze static error parameters.

$W_{n/n-1}\delta\underline{X}_{o/o}$ = component due to errors in the initial state.

$\underline{b}_{n/n-1}$ = component due to zero mean state noise.

$\underline{g}_{n/n-1}$ = component due to zero mean measurement noise.

Under this assumption, the total a priori state covariance matrix is given by

$$V_{n/n} = L_{n/n-1}\ S\ L^{T}_{n/n-1} + W_{n/n-1}\ P_{o/o}\ W^{T}_{n/n-1} + F_{n/n-1} + G_{n/n-1}$$

In SEAMAP the last 3 components of $V_{n/n-1}$ are grouped as

$$P_{n/n-1} = W_{n/n-1}\ P_{o/o}\ W^{T}_{n/n-1} + F_{n/n-1} + G_{n/n-1}$$

At time t_n the force model subroutines (see flow chart Figure (2.1)) evaluate $\underline{X}_{n/n-1}$ and $\Phi_{n,n-1}$ using the previously estimated state $\underline{X}_{n-1/n-1}$. These quantities are then used to update the unmodeled analyze coefficient matrix.

$$L_{n/n-1} = \Phi_{n,n-1}\ L_{n-1/n-1}$$

The state covariance components due to initialization errors, state noise and sensor noise are updated as

$$P_{n/n-1} = \Phi_{n,n-1}\ P_{n-1/n-1}\ \Phi^{T}_{n,n-1} + Q_n$$

The sensor model subroutines then evaluate the measurement residual, $\delta\underline{y}_n$, the partial derivatives of the measurement with respect to the adjusted parameters, M_n, the partial derivatives of the measurement with respect to unadjusted analyze parameters, A_n, and the measurement noise covariance matrix R_n.

The residual covariance matrix is computed as

$$C_n = E\ (\delta \underline{y}_n\ \delta \underline{y}_n^T) = M_n\ P_{n/n}\ M_n^T + R_n$$

A chi square statistic, ε_n, is computed to test the consistency of the residual, $\delta \underline{y}_n$, with its analytically computed covariance matrix, C_n. If ε_n is above some preset threshold, the editing logic is activated; otherwise, the measurement residual is used to adjust the state vector. The adjust gain is computed as:

$$K_n = P_{n/n-1}\ M_n^T\ C_n^{-1}$$

The rows of K_n corresponding to consider parameters are filled with zeroes and the adjustment is given by

$$\underline{X}_{n/n} = \underline{X}_{n/n-1} + K_n\ \delta \underline{y}_n$$

Using the above gain matrix (with consider rows zeroed) the unadjusted analyze coefficients are updated as:

$$L_{n/n} = (I - K_n M_n)\ L_{n/n-1} - K_n A_n$$

And the after adjustment state covariance matrix is computed as

$$P_{n/n} = (I - K_n M_n)\ P_{n/n-1} (I - K_n M_n)^T + K_n R_n K_n^T$$

For display purposes the total state covariance matrix, including the effects of uncertainties in the unadjusted analyze parameters is computed as:

$$V_{n/n} = P_{n/n} + L_{n/n} \; S \; L_{n/n-1}^{T}$$

2.3 DATA EDITING LOGIC

Each measurement residual vector is compared with the analytically computed residual covariance matrix by computing the statistic

$$\varepsilon_n = \delta \underline{y}_n^T \; C_n^{-1} \; \delta \underline{y}_n$$

Under the assumptions used to derive the sequential filter ε_n follows a chi square distribution with degrees of freedom equal to the number of elements in the measurement vector $\underline{y}_n$. This statistic is scale free (i.e., independent of the measurement units such as meters, seconds, degrees, etc.) and the significance levels depend only on the number of degrees of freedom.

A very large value of ε_n may be due to

1. A single outlying measurement.

2. Use of incorrect noise statistics within the measurement model.

3. An unmodeled state disturbance.

The data rate was very high (1/second) in comparison to the response time of the Vanguard to unmodeled forces. Because of the redundancy of ground truth quality sensors it was possible to verify the measurement error statistics for each sensor. Therefore in reducing the MANSEE data it was assumed that large values of ε_n were only caused by outlying measurements.

Whenever a large value of ε_n is detected the components of δy_n are compared with their standard deviations. Those components outside the ± 3 sigma points are deleted from the current measurement. The threshold value is input for each sensor.

Definition of Symbols

$\underline{X}_{k/j}$ = State vector of adjusted parameters

$\underline{s}$ = Vector of sensor model static error parameters (assumed zero mean)

$\underline{Y}_i$ = Measurement vector

$\underline{Y}_{i/j}$ = Anticipated measurement vector

$\underline{f}_i$ = Nonlinear vector function giving state vector at time i as a function of state vector at some earlier time

$\underline{m}_i$ = Nonlinear vector function giving the anticipated measurement as a function of the current state, $\underline{X}_i$ and of the sensor static error parameter $\underline{s}$

$\Phi_{i,j}$ = State transition matrix computed in the force model subroutines

$L_{i/j}$ = Sensitivities of the adjusted parameters wrt the sensor static error parameters ($\underline{s}$)

S = $E(\underline{s}^T \underline{s})$

$V_{i,j}$ = Total state covariance matrix

Q_i = State noise covariance matrix

R_i = Sensor noise covariance matrix

$\delta \underline{Y}_i$ = Measurement residual

M_i = Partial derivatives of the measurement wrt the vector of adjusted parameters ($\underline{X}_i$)

A_i = Partial derivatives of the measurement wrt the unadjusted sensor static error parameters ($\underline{s}$)

C_n = Residual covariance matrix

K_n = Filter gain matrix

ε_n = Residual chi square statistic

ε_T = Rejection threshold for current sensor

Q_o = Nominal state noise covariance matrix

$\underline{b}_{i/j}$ = Component of state error due to zero mean state noise

$F_{i/j}$ = Component of state covariance matrix due to zero mean state noise

$G_{i/j}$ = Component of state covariance matrix due to zero mean state noise

$P_{i/j}$ = State covariance matrix not including effects of unmodeled analyze parameters.

REFERENCES

1. Johnson, D.J., "A General Linear Sequential Filter, AIAA Journal, Vol. 8, No. 9, September 1970.

2. Hatch, W.E., Final Report for the Design of Prototype Attitude Determination Software for the RAE-B Satellite, Feb. 1972, Wolf Research and Development Corporation, Contract No. NAS 5-11736 - MOD 120.

SECTION 3.0
MEASUREMENT MODELS

SEAMAP currently includes measurement models for the following sensor types:

1. Ship velocity $(\dot{x},\dot{y})$
2. Ship position (ϕ,λ)
3. Land based radar (R,A_z)
4. Ship based radar (R,A_z)
5. Range only (R)
6. LORAN-C $(\Delta t_1, \Delta t_2)$
7. Hyperbolic Lane Count $(\Delta \ell_1, \Delta \ell_2)$
8. Ship heading (C_t)

The program is designed so that additional sensor types can be included without disturbing any of the existing code.

As described in Section 2.0 each sensor measurement is related to the system state by the nonlinear vector equation:

$$\underline{y}_i^k = \underline{M}_i \left(\underline{X}_i^d, \underline{X}_i^k, \underline{s}^k\right) + \underline{r}_i^k$$

where

$\underline{X}_i^d$ = force model parameters which are ship latitude, longitude, east velocity and north velocity.

$\underline{X}_i^k$ = static parameters of the k^{th} sensor which are to be adjusted or treated as consider parameters.

$\underline{s}^k$ = static error parameters of the k^{th} sensor which are treated as unmodeled analyze parameters.

$\underline{r}_i^k$ = zero mean measurement noise vector.

The sensor subroutines compute a priori values of $\underline{y}_i^k$ and the partial derivatives of $\underline{y}_i^k$ with respect to $\underline{x}_i^d$, $\underline{x}_i^k$ and $\underline{s}^k$.

3.1 SHIP VELOCITY MEASUREMENT MODEL

SINS measures ship east and north velocity. In addition to random errors it is assumed that each measurement contains an offset error plus a bias that varies linearly with time. Thus the a priori velocity measurements are modeled as:

$$y_1 = \dot{x} + \alpha_1 + \beta_1 \Delta t + r_1$$

$$y_2 = \dot{y} + \alpha_2 + \beta_2 \Delta t + r_2$$

where:

$\dot{x},\dot{y}$ = actual east and north velocities.

α_1,α_2 = east and north offset errors.

β_1,β_2 = linear bias coefficient.

r_1,r_2 = zero mean random noise terms.

Δt = time since filter initialization.

3.2 SHIP POSITION MEASUREMENT MODEL

Direct measurements of ship latitude and longitude are obtained from SINS, AN/SRN-9 and the Marine STARTRACKER. In addition to random noise it is assumed that each measurement contains an offset error plus a bias that varies linearly with time. The a priori measurements are modeled as:

$$y_1 = \phi + \alpha_1 + \beta_1 \Delta t + r_1$$

$$y_2 = \lambda + \alpha_2 + \beta_2 \Delta t + r_2$$

where:

ϕ, λ = actual latitude and longitude.

$\alpha_1, \alpha_2, \beta_1, \beta_2, r_1, r_2, \Delta t$ are defined as above.

3.3 LAND BASED RADAR MODEL

The land based radar measures range and azimuth to a ship mounted transponder. Each of these measurements contains a constant bias plus random noise. In addition the station location is subject to survey errors. Thus the radar measurements are given by:

$$y_1 = R(\phi, \lambda, \phi_s, \lambda_s, \Delta\phi_s, \Delta\lambda_s) + \Delta R + r_1$$

$$y_2 = A(\phi, \lambda, \phi_s, \lambda_s, \Delta\phi_s, \Delta\lambda_s) + \Delta A_Z + r_2$$

where.

ϕ,λ = ship latitude, longitude.

ϕ_s,λ_s = station latitude, longitude.

$\Delta\phi_s,\Delta\lambda_s$ = station location survey errors.

$\Delta R,\Delta A_Z$ = Range, azimuth bias errors.

r_1, r_2 = random measurement noise.

Range, azimuth and the appropriate partial derivatives are computed within subroutine ARC.

3.4 SHIP BASED RADAR

The ship based radar measures range and azimuth relative to the ships bow of a transponder on shore. These measurements are assumed to contain a constant bias plus noise. The location of the transponder is subject to survey errors. Thus the a priori ship radar measurement is computed as:

$$y_1 = R(\phi,\lambda,\phi_T,\lambda_T,\Delta\phi_T,\Delta\lambda_T) + \Delta R + r_1$$

$$y_2 = A(\phi,\lambda,\phi_T,\lambda_T,\Delta\phi_T,\Delta\lambda_T) - \text{ATAN}\ (\dot{x}/\dot{y}) + \Delta A_Z + r_2$$

where:

ϕ_T, λ_T = transponder latitude, longitude

$\Delta\phi_T, \Delta\lambda_T$ = transponder location survey error

$\dot{x}$ = ship east velocity

$\dot{y}$ = ship north velocity

and the remaining symbols are defined as above.

Range, azimuth and the appropriate partial derivatives are computed within subroutine ARC.

3.5 LORAN-C

LORAN-C is a pulsed hyperbolic positioning system. The measurements are the differences in arrival time between a master pulse and the pulses from each of two slave stations. The station locations are subject to survey errors. Each time difference measurement contains a bias term which is the sum of secondary phase correction errors and interstation delay errors. The index of refraction is also treated as a systematic error parameter.

The LORAN-C measurements are modeled as:

$$y_1 = \frac{n}{c}\left(R_{s_1} - R_m + R_{ms_1}\right) + E_{s_1} - E_m + E_{s_1 m} + D_{ms_1} + r_1$$

$$y_2 = \frac{n}{c}\left(R_{s_2} - R_m + R_{ms_2}\right) + E_{s_2} - E_m + E_{s_2 m} + D_{ms_2} + r_2$$

where

c = velocity of light in vacuum

n = index of refraction (n=1.000338)

R_{s_1}, R_{s_2} = ranges from ship to slave #1, slave #2

R_m = range from ship to master station

R_{ms_1}, R_{ms_2} = ranges from master to slave #1, slave #2

E_{s_1}, E_{s_2} = secondary phase corrections for slave #1, slave #2

D_{ms_1}, D_{ms_2} = fixed delay between reception of master pulse and transmission of slave pulse for slave #1, slave #2.

r_1, r_2 = zero mean measurement noise.

The values for $E_{s_1}, E_{s_2}, E_m, E_{s_1m}, E_{s_2m}$ are computed analytically assuming propagation over seawater[1].

R<100 statute miles (161 Km)

$$E = 821.544/R - .011402 + 1.0936\times10^{-6} R$$

R≥100 statute miles (161 Km)

$$E = 38673.4/R - 0.40758 + 2.15476\times10^{-6} R$$

where R is in meters.

---

[1] Winkler, G.M.R., "Path Delay, Its Variations, and Some Implications for the Field Use of Precise Frequency Standards," Proceedings of the IEEE, Vol. 60, No. 5, May 1972.

In addition to the secondary phase correction E, there is another correction which takes into account the fact that propagation may be over land rather than over seawater. This correction (called the ASF) must be computed for each pair of stations at the particular position of interest. Values obtained from the U.S. Coast Guard for the MANSEE test area are:

Channel Y: ASF = -1.229 μsec

Channel Z: ASF = +2.088 μsec

For simplicity, these numbers are combined with the fixed delay between stations so that the values used for D are:

Channel Y: D_{sm_1} = 49000.-1.229=48998.771 μs

Channel Z: D_{sm_2} = 65000.+2.088=65002.088 μs

These measurements and the appropriate partial derivatives are computed within subroutine LORP.

3.6 HYPERBOLIC LANE COUNT MEASUREMENTS

Hyperbolic lane count measurements are obtained from OMEGA and RAYDIST. These systems are similar to LORAN-C except that the basic measurement is the phase difference between two CW signals rather than the arrival time difference for two pulses. A lane count measurement is ambiguous in that the measuring receiver only establishes position within a lane. (One lane = $\lambda/2$ meters where λ is the continuous wave length.) Thus the actual measurement is some fraction of a lane. The integer lane count is arbitrarily set at the beginning of a navigation exercise and is updated either manually or automatically each time and the receiver records a lane crossing.

SEAMAP obtains the initial integer lane count from an input parameter card. As a default option this integer count is taken to be the integer part of the first lane count measurement processed. OMEGA and RAYDIST station locations are subject to survey error. Lane count measurements contain bias errors which are the sum of the secondary correction errors for each station. The phase velocity is also treated as a systematic error parameter.

Within SEAMAP, a priori lane count measurements are computed by first computing the arrival time differences and then converting these differences to lane counts. Thus the lane count is given by:

$$y_1 = \frac{f}{v}(R_{A_1} - R_{B_1}) + E_{A_1} - E_{B_1} + r_1 + \ell_{o_1}$$

$$y_2 = \frac{f}{v}(R_{A_2} - R_{B_2}) + E_{A_2} - E_{B_2} + r_2 + \ell_{o_2}$$

where:

v = phase velocity

R_{A_1}, R_{B_1} = distances from ship to channel 1 stations

R_{A_2}, R_{B_2} = distances from ship to channel 2 stations

f = CW transmission frequency

E_{A_1}, E_{B_1} = Channel 1 secondary phase corrections

E_{A_2}, E_{B_2} = Channel 2 secondary phase corrections

r_1, r_2 = zero mean measurement noise

ℓ_{o_1}, ℓ_{o_2} = lane count origin adjustment

For OMEGA, v was assumed to be 300574000 and f was 10.3 KHz. The predicted propagation corrections (E_{A_1},E_{A_2},E_{B_1},E_{B_2}) for OMEGA are tabulated by the Defense Mapping Agency Hydrographic Center. Figures A-1 and A-2 are plots of the propagation correction for the MANSEE test area during early June 1972 for stations B,C,D and F. At the time of the test, station D was located in Forrest Port, New York and station F was in North Dakota. Both stations were operating on temporary assignments.

The secondary phase corrections for Raydist were assumed to be zero due to the shorter distances involved. v was assumed to be 299670000 and f was 3.307400 MHz (Red Channel) and 3.307550 MHz (Green Channel). These a priori measurements and the appropriate partial derivatives are computed within subroutine MELCNT.

3.7 HEADING MEASUREMENTS

Ship heading relative to north is measured by SINS and the MK-19 gyrocompass. In addition to random errors it is assumed that heading measurements contain an offset plus a bias that varies linearly with time. Thus the a priori heading measurement is given as:

$$C_r = \text{ATAN}\ (\dot{x}/\dot{y}) + \alpha + \beta\ \Delta t + r$$

where:

$\dot{x},\dot{y}$ = actual east, north velocities

α,β = offset and time linear term

r = random measurement noise

This measurement and the appropriate partial derivatives are computed within subroutine MEHEAD.